

Diffusion in energy materials: Governing dynamics from atomistic modelling

D. Parfitt, A. Kordatos, P. P. Filippatos, and A. Chroneos

Citation: [Applied Physics Reviews](#) **4**, 031305 (2017);

View online: <https://doi.org/10.1063/1.5001276>

View Table of Contents: <http://aip.scitation.org/toc/are/4/3>

Published by the [American Institute of Physics](#)

Articles you may be interested in

[Cathodoluminescence for the 21st century: Learning more from light](#)
[Applied Physics Reviews](#) **4**, 031103 (2017); 10.1063/1.4985767

[Mechanical behaviors of nanowires](#)
[Applied Physics Reviews](#) **4**, 031104 (2017); 10.1063/1.4989649

[Bending induced electrical response variations in ultra-thin flexible chips and device modeling](#)
[Applied Physics Reviews](#) **4**, 031101 (2017); 10.1063/1.4991532

[InAs/GaSb type-II superlattice infrared detectors: Future prospect](#)
[Applied Physics Reviews](#) **4**, 031304 (2017); 10.1063/1.4999077

[Porous Si as a substrate for the monolithic integration of RF and millimeter-wave passive devices \(transmission lines, inductors, filters, and antennas\): Current state-of-art and perspectives](#)
[Applied Physics Reviews](#) **4**, 031102 (2017); 10.1063/1.4998965

[Electromigration and the structure of metallic nanocontacts](#)
[Applied Physics Reviews](#) **4**, 031302 (2017); 10.1063/1.4994691

Diffusion in energy materials: Governing dynamics from atomistic modelling

 D. Parfitt,^{1,a)} A. Kordatos,¹ P. P. Filippatos,² and A. Chroneos^{1,3,b)}
¹*Faculty of Engineering, Environment and Computing, Coventry University, Priory Street, Coventry CV1 5FB, United Kingdom*
²*Department of Electrical and Computer Engineering, National Technical University of Athens, 9 Iroon Polytechniou str., Zografou 157 80, Greece*
³*Department of Materials, Imperial College London, London SW7 2AZ, United Kingdom*

(Received 31 December 2016; accepted 18 July 2017; published online 12 September 2017)

Understanding diffusion in energy materials is critical to optimising the performance of solid oxide fuel cells (SOFCs) and batteries both of which are of great technological interest as they offer high efficiency for cleaner energy conversion and storage. In the present review, we highlight the insights offered by atomistic modelling of the ionic diffusion mechanisms in SOFCs and batteries and how the growing predictive capability of high-throughput modelling, together with our new ability to control compositions and microstructures, will produce advanced materials that are designed rather than chosen for a given application. The first part of the review focuses on the oxygen diffusion mechanisms in cathode and electrolyte materials for SOFCs and in particular, doped ceria and perovskite-related phases with anisotropic structures. The second part focuses on disordered oxides and two-dimensional materials as these are very promising systems for battery applications. *Published by AIP Publishing.* [<http://dx.doi.org/10.1063/1.5001276>]

TABLE OF CONTENTS

I. INTRODUCTION	1
A. Technological motivation	2
II. DIFFUSION MECHANISMS	3
A. Defect formation	3
B. Defect mobility	4
III. ATOMISTIC SIMULATION METHODOLOGY	5
A. Electronic structure methods	5
B. Empirical potentials	6
C. Estimating diffusion from molecular dynamics (MD)	6
D. Estimating diffusion from molecular statics	7
IV. OXYGEN DIFFUSION MECHANISMS IN SOFCs	8
A. Doped-ceria	8
B. Perovskites	10
C. Layered perovskites	11
D. Apatite-based materials	12
E. Concluding remarks	13
V. LITHIUM DIFFUSION MECHANISMS IN BATTERIES	14
A. Li_xCoO_2 and related compounds	14
B. Phosphate based cathodes	16
C. Electrolyte developments	16
D. MXenes	17
VI. SUMMARY AND CONCLUSIONS	18

A. Strain and interface design	18
B. Computational material discovery	19
C. Concluding remarks	19

I. INTRODUCTION

One of the key challenges facing our community is the production of better materials for the generation, transport, and storage of energy. New materials are needed to develop existing and enable future technologies that will allow energy to be used in a cleaner, more sustainable manner. In this review, we consider the contribution of atomic scale modelling of diffusion, specifically in materials that are part of an electrochemical cell, as a battery or a solid-oxide fuel cell. This is motivated primarily by the increasing importance of these components in our energy infrastructure, but there is also an opportunity due to the current investment, to exploit and develop broader concepts of the way materials may function. We will discuss the use of modelling to understand, and through the growth in computing power, to predict diffusion and how this will ultimately allow the design of novel compositions or microstructures to optimise properties in a particular environment. The commercial and engineering interest and the (relatively) high level of solid-state diffusion in these materials mean that a wide range of computational approaches have been successfully applied and accompanied by a wealth of experimental data. This therefore offers a template for how research in other areas may also evolve.

Diffusion is a fundamental process in solid state physics that, despite being mathematically simple in its formulation,

^{a)}Electronic mail: david.parfitt@coventry.ac.uk

^{b)}Electronic mail: ab8104@coventry.ac.uk

is fiendishly complex when required to be predictive in real applications. This complexity emerges from the range of time and length scales that in concert determine the bulk behaviour of a material. Of these different time and length scales, in this review we discuss the insights available from atomistic modelling and simulations. Diffusion in the solid state is intrinsically an atomic process, requiring the transport of species essentially atom-by-atom from one side of an electrochemical cell to the other. It is unsurprising that atomic parameters influence diffusion. Beneath this, however, is a more fundamental reason for the atomic scale: Diffusion is difficult to predict because details of the motion of atoms are coupled to bulk properties, such as temperature and stress, and to the microstructure and composition of a material; there is, however, very little physics at length or timescales smaller than an atom that needs to be included. The motion of electrons occurs on timescales so divorced from the motion of atoms in a solid that we can consider the electrons to be predominantly in their lowest energy configuration.^{1,2} Similarly, the process of diffusion, with the exception of a few special cases,³ is bereft of concerns over the isotopic makeup of a given element's nucleus. This break with lower length scales provides a natural base for our discussion of diffusion and means that we may capture our understanding using non-relativistic quantum mechanics, one of the most powerfully predictive theories that we have available.

The great difficulty in basing our models in the atomic scale is of course that most components have a great number of atoms and that these atoms move quickly and in ways that are coupled to the position of other atoms, both in their immediate neighbourhood and the broader microstructure of a material. Two approaches have emerged to address this. The first is multiscale modelling where the details of atomic diffusion are contained but abstracted within higher length scale models, which may include chemical concentrations, reaction rates, temperature, or stress. In principle, a deep dive into these models will recover the diffusion process with full atomic-scale fidelity but coupled to the conditions and environment at a specific location. This allows the mimicry of devices with realistic environmental conditions and material heterogeneity. Its success depends on the tremendous progress made in both computational power, and equally important, the elegance with which we can pose questions to and understand answers from our computers.

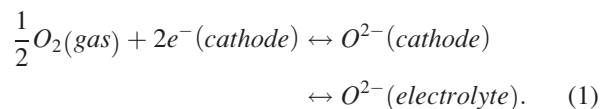
The second approach, which we concentrate on in this review, is the use of atomic scale calculations to understand and optimise diffusion in energy materials by direct comparison to experiment or application *without* recourse to a sequence of higher length scale models. These data are a subset of the multiscale approach, but the philosophy is sufficiently different to merit individual consideration. The advantages over the multiscale approach are that the simulations are much more modest in their scope and therefore a greater number of calculations can be performed. Combined with the emphasis on understanding the diffusion process, this allows predictions and empirical models to be developed that may outperform larger length scale simulations. In the field of energy, and increasingly across much of engineering,

materials with considerable compositional or structural flexibility are being proposed and there is a dire need for rational design rules to help target chemical synthesis. An emerging trend in this field is the use of high-throughput simulations together with large-scale data analysis to profile a whole region of composition or structural space in order to predict the properties of new, uncharted compounds.^{4,5}

As examples of the use of atomic scale simulations we select two current challenges of great technological importance to the energy sector: improving diffusivity in intermediate temperature solid oxide fuel cells (SOFCs) and solid state battery cathodes and electrolytes. This is motivated by their current commercial interest but also because the high levels of diffusion make the physics of diffusion more directly accessible in these materials. For both of these applications, and for several specific classes of materials within them, we highlight examples of the atomic scale simulations that have been performed, what insights have been proposed of the dynamics of diffusion and where these insights have had an impact in improving or developing materials.

A. Technological motivation

The importance of SOFCs is their potential for high efficiency energy conversion accompanied by reduced emission of greenhouse gases as compared to fossil-fuel based power generation.^{6,7} For high operating temperatures (up to 1000 °C), SOFCs can operate with hydrogen and/or natural gas efficiently converting the chemical energy to electricity (for example, in combined heat and power applications) but the high operating temperatures can result in materials issues and increased cost.^{8–11} In particular, high temperatures lead to thermal cycling, performance degradation, and the use of expensive materials in interconnects.¹⁰ To alleviate these issues, the community aims to lower the operating temperatures of SOFCs to the intermediate temperature range (500–700 °C).^{11–13} Regrettably, however, this reduction in temperature leads to an increase in the losses for reaction and transport kinetics in the active layers of the SOFC, and in particular, the cathode and electrolyte. This has led to the search for new classes of materials that have high oxygen diffusivities at 500–700 °C. Oxygen diffusivities are important as in the intermediate temperature range the oxygen reduction reaction in the cathode and the oxygen transport in the cathode and electrolyte need to be accelerated. This is summarized by the following reaction:



The first part stands for the reduction of oxygen on the cathode surface, whereas the second and third reactions represent the diffusion of oxygen in the cathode and electrolyte, respectively. These reactions have high activation energies in conventional SOFC materials (for example, as La_{1-x}Sr_xMnO_{3-δ}) and consequently, a temperature decrease will result in significant electrical energy losses.¹⁴ In that respect, mixed ionic-electronic conductors (MIEC) have been

considered in previous studies,^{14–17} which determined that the oxygen reduction kinetics in these MIEC electrodes is contributed by both the oxygen surface exchange and diffusion. Oxygen diffusion is also important for electrolytes but it should be accompanied by low electronic conductivity.

The second example considered in the present review is materials for cathodes and solid electrolytes for battery applications. Solid-state rechargeable Li-ion batteries have already attracted significant scientific investment due to their high capacities and energy densities. The solid electrolyte is an important component of the battery,¹⁸ with both theoretical and experimental studies focusing on the advanced research of new systems. A key idea is to effectively increase the ionic conductivity at the operation temperature by replacing the solvent electrolytes with new solid materials in order to exceed the restrictions that emerge in the case of electrochemical applications.^{18,19} Furthermore, the electrolyte has to be compatible with the electrode materials which are used for the charge and discharge procedures, a fundamental need for the device operation as the ions are released and reinserted for hundreds of times during the battery life cycle.²⁰

In both examples, the dynamics of ionic diffusion can be affected and tuned by the crystal structure, composition, doping, and elastic strain. Atomic scale modelling can offer a direct way to gain detailed insight for the formation and diffusion of defects in numerous inorganic materials of technological importance.^{21,22} In conjunction with related experiments, atomistic modelling can provide a direct route to uncover the governing dynamics of SOFCs and battery materials.

This review is structured as follows: First, we summarise the relevant diffusion mechanisms in solid state materials and then discuss the two dominant atomistic scale methodologies, density functional theory (DFT) and parameterised potentials. Then, we consider cathode and electrolyte SOFC materials focusing on doped-ceria, the Ruddlesden-Popper series of layered perovskites, and silicate and germanate based apatite minerals. This is followed by the discussion of lithium diffusion in partially disordered oxides such as lithium lanthanum titanates (for example, $\text{La}_{2/3-x}\text{Li}_{3x}\text{TiO}_3$, LLTO) and two-dimensional materials such as MXenes. Finally, we summarise and present future directions to optimise the ionic diffusion and to discover new structures and compositions using atomic-scale modelling.

II. DIFFUSION MECHANISMS

Diffusion in ionic materials is complex due to the presence of distinct cation and anion sublattices. Generally, diffusion of both ion types is limited to their own sublattice; however, the opposite sublattice often has a controlling influence on the overall level of diffusion, both directly during the migration process and indirectly through control of the number and character of the mobile species.

For net diffusion to occur in a crystalline material, atoms must migrate away from their equilibrium positions into neighbouring sites. In some special cases, this is achieved through a total loss of the short range order on one of the ionic sublattices (so-called Type-I superionics^{23,24});

however, the transformation to this distinct phase is often accompanied by a discontinuity in the cell volume that would prove problematic for device performance. In the materials considered here, bulk diffusion is accommodated through the individual or cooperative migration of point defects (interstitials and/or vacancies). The overall diffusivity of a material is made up of effectively two parts (a) the formation and stability of these charged species and (b) the factors affecting the mobility of these defects within the lattice.

A. Defect formation

At a finite temperature, all materials contain point defects and their number and concentration are determined by the temperature, the chemistry and crystallography of the host lattice and the external environment. For example, the classic Frenkel pair formation in a simple binary oxide like MgO occurs via the reaction



where we use the Kroger-Vink notation²⁵ to describe the appearance of the doubly charged vacancy and interstitial in the host lattice. The concentration of these species is determined by the law of mass action and the defect formation energy E_f

$$\frac{[\text{O}_\text{i}][\text{V}_\text{O}]}{[\text{O}_\text{O}]} = \exp\left(-\frac{E_f}{k_b T}\right), \quad (3)$$

where [...] denotes the concentration of each species at a temperature T . Equation (3) introduces a strong temperature dependence of the defect concentration (and the thermal concentrations of point defects in many materials are consequently very low unless close to the melting point) but much important physics is also hidden within this definition of the formation energy. It depends not just on the change in the potential energy of a configuration of atoms, a quantity that is (relatively) straightforward to calculate on an atomic scale, but also on the differences in vibrational energy, electronic and vibrational entropy, the external chemical potential, and the difference in volume between the defective and perfect crystal. These are thermodynamically well defined properties, but how to practically calculate or approximate them from atomic scale simulations has only recently been possible.²⁶

Point defects may come from both intrinsic and extrinsic sources. In the intrinsic case, non-stoichiometry may be accommodated through reduction of one or more metal ions to provide charge compensation, and transition metal (TM) or lanthanide oxides are particularly favourable for this mechanism. For example, the reduction of Ce^{4+} to Ce^{3+} ions in CeO_2 (Ref. 27) can provide a significant population of intrinsic oxygen vacancies at high temperatures. These reduction reactions however often come with an increase in electronic conductivity; in the case of CeO_2 the additional electron and surrounding lattice distortion (a polaron) is itself mobile and can hop between Ce sites. This may be acceptable for electrode materials but unsuitable for

electrolytes where it would provide a short circuit between the two sides of the cell.

In the absence of any intrinsic charge compensation mechanism, useful levels of diffusion in ionic materials can also be achieved through the introduction of aliovalent dopants into an ionic lattice.²⁸ These stabilize an athermal concentration of charge compensating point defects (either vacancies or interstitials) which may be controlled by the level and type of dopant ion. For example, the solution of yttrium into ZrO_2 to form yttria-stabilized zirconia (YSZ) produces half as many $2+$ charged oxygen vacancies as there are Y^{3+} ions onto a Zr^{4+} host site.

B. Defect mobility

A high concentration of charge carriers is necessary for useful levels of diffusion; however they must also be sufficiently mobile within the lattice. For many point defects, the mobility is well approximated by harmonic transition state theory,²⁹ in which the frequency of site-to-site hops, ν , at a temperature T is given by

$$\nu = \nu_0 \exp\left(-\frac{E_m}{k_b T}\right), \quad (4)$$

where E_m is a migration energy for a given transition, and within harmonic transition state theory, ν_0 is the ratio of product sums of the vibration frequencies at the minima and saddle point.

Using an oxygen-vacancy assisted diffusion process as an example, this leads to a diffusivity

$$D_v = [V_O] f \lambda^2 \nu_0 \exp\left(-\frac{E_m}{k_b T}\right), \quad (5)$$

where λ is the distance of each ion hop and f is a geometry factor that represents the number of possible diffusion pathways. It follows that for most materials, diffusion at a given temperature is determined by the concentration of mobile defects and the smallest activation energy, E_m , that is consistent with bulk mobility. This is an important simplification as it means that of the myriad of possible routes for an ion to move through a material, the one that actually matters is the one with the lowest migration energy as this will have a dominating influence on the bulk diffusivity. A corollary to Eq. (5) is the observation that in cases where the $[V_O]$ term in Eq. (5) is generated just from the exponential term in Eq. (3), diffusion is only observed where sufficient populations of intrinsic defects exist (for example, at high temperatures). At lower temperatures, either an extrinsic population of defects or reduction of a host ion is required to promote useful ionic diffusion.

From Eq. (5), we may naively suppose that, as well as higher dopant levels being beneficial to diffusivity, broadly the increase should be linear with dopant ion concentration. This is not generally true: the presence of a non-dilute level of dopants may change both the migration energy through effects such as chemical expansion^{30,31} and the overall migration pathway. We show an example in Fig. 1 of an abstract, two-dimensional lattice containing two aliovalent

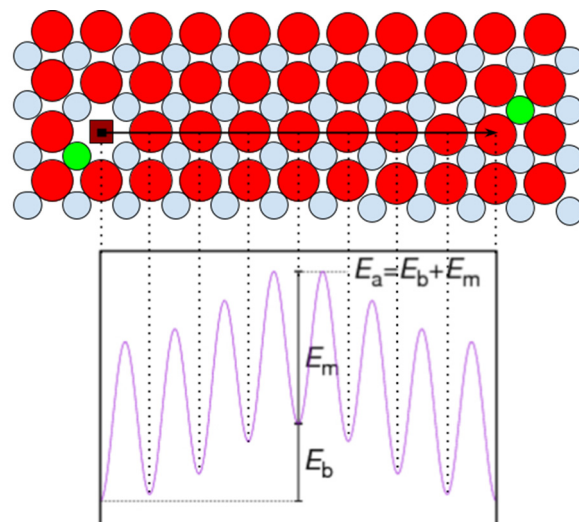


FIG. 1. Illustration of a vacancy diffusion mechanism with an overall activation energy of E_a composed of the basic migration energy, E_m , plus the energy needed to separate the ion from a dopant to enable long range diffusion.

dopants and an associated lattice vacancy. Although the individual lattice hops have similar migration energies (and these may or may not be altered by the presence of the dopant), bulk diffusivity requires an extended network of accessible sites and therefore we must include movement of ions to and away from the dopants. This introduces an activation energy, E_a , that is the sum of the migration energy, E_m , and a binding energy, E_b , required to separate the point defect from the dopant ion. The overall effect is a complicated function of this binding energy and the concentration of the dopants: Very low dopant concentrations reduce the number of available point defects but may mean that the ions are infrequently trapped and highly mobile, particularly when this is coupled with relatively low binding energies; conversely, high dopant concentrations may allow the numerous point defects to accomplish long range diffusion without ever leaving the sphere of influence of the dopant ions.

What features of a crystal lattice are useful in promoting high levels of diffusivity of ions? A common route to establish high levels of diffusivity will be through doping in some way to provide an athermal concentration of point defects. For this to occur, the lattice must be tolerant of both the dopant ion and the resultant defects, which favours structures with highly polarisable ions and soft elastic modes. These allow the long-range Coulomb interaction between interstitials or vacancies to be effectively screened and the local ion relaxation around point defects to be amortised through an extended structural relaxation, for example, the channel expansion in apatites,³² the twisting of iodide tetrahedra in silver rubidium iodide,³³ or the titling of the octahedra in perovskites.³⁴

As well as a significant concentration of charge carriers these species must also be mobile within the crystal lattice, i.e., we would like to minimise E_m in Eq. (5). During the migration process, the mobile ion will pass through non-ideal coordination with its surrounding ions. Ions which are either small or highly polarisable are therefore favoured due

to their ability to squeeze through smaller gaps in the surrounding structure.^{35–37} Good ionic conductors also often adopt a rich variety of polytypes as a function of pressure, temperature, or composition; this structural agnosticism is linked to the ability to provide the low energy pathways, a network of partially occupied sites and the ability to locally distort in order to ease the passage of the mobile ion [for example, the percolation and paddle wheel mechanisms proposed in Li_2SO_4 (Ref. 38)].

III. ATOMISTIC SIMULATION METHODOLOGY

As the focus of the present review is diffusion in energy materials we will briefly introduce the two common approaches to atomic scale modelling of these materials: density functional theory (DFT) methods and parameterised potential forms, noting the differences in approach between the two. We shall also discuss the use of these methods in calculating bulk diffusivity.

A. Electronic structure methods

A quantum mechanical formulation offers the most complete description of atomic interactions in the solid state; however, the analytical or direct numerical solution of Schrödinger's equation is intractable for greater than a handful of atoms because of the correlations between the multiple electrons. DFT recasts the problem of many interacting electrons and nuclei to a single particle Kohn-Sham expression³⁹ which assumes that (i) the total energy (or in fact any ground state property) of a system of electrons is written as a unique functional of the total electron density, and (ii) the variational minimum of this total energy is exactly equivalent to the true ground state energy. This is a huge simplification and has been crucial in the adoption of the technique for a wide range of solid state calculations.

The central tenant of DFT, which replaces the complex, interacting set of electron wavefunctions with a functional of single scalar field, is exact; finding a suitable set of functionals that represent the exchange correlation however requires an approximation. The success of DFT in describing solid state systems is due to the ability of relatively unsophisticated functionals to predict bulk properties with remarkable accuracy. For example, the local density approximation (LDA) introduced with the original Kohn-Sham expressions³⁹ derives the exchange-correlation functional by assuming that each infinitesimal element of density contributes an exchange-correlation energy equal to that of a uniform electron gas.⁴⁰ The charge density around atomic cores is highly non-uniform and therefore, the approximation is unjustified on any physical basis other than it works and it works for a huge variety of different systems. The generalised gradient approximation (GGA) was introduced specifically to recognise some of the shortcomings of the LDA by allowing the exchange energy to vary with the gradient of the electron density and gives better replication of some binding and dissociation energy (particularly for those containing hydrogen).^{41–43}

The physics of the calculation is fixed by the choice of the exchange functional. Many further parameters can degrade

the accuracy of the calculation (and often this is an appropriate tradeoff for computational expediency) but never replace the physics absent from the original formulation. The use of the LDA or GGA is a reasonable starting point for many solid state calculations and is often entirely sufficient to predict gross trends across different substitutional elements. However, a number of further functionals have been proposed which reintroduce some of the physics absent from the LDA or GGA treatments⁴⁴ for a range of chemical and solid state problems. Of greatest importance for the treatment of diffusion in energy materials is the handling of compounds doped with rare earth or transition metals using either hybrid functionals or the Hubbard model. Hybrid functionals improve the estimates of the ground state energy through an admixture of the traditional DFT functional and an estimate of the exact exchange energy calculated from Hartree Fock theory⁴⁵ but using a common electron density for the two expressions. The Hubbard model, often described as “DFT + U”, introduces an energy correction term (which may be empirically fitted to a band gap) for both the Coulomb and exchange energies of localised electrons that biases the calculation to favour either fully occupied or unoccupied energy levels.⁴⁶ Both of these approaches are extremely important in replicating the band structure of many important transition or rare-earth metal compounds^{47,48} because the higher angular momentum *d*- and *f*-orbitals in these elements are more strongly localised around the atomic core and there is a greater consequence of the neglect of electron-electron interactions in the Kohn-Sham expression. Obtaining the correct band structure in these cases may have a direct effect on the accuracy of the calculated defect energies.⁴⁹ The use of these variations in the original LDA or GGA is not without difficulty, however, particularly when considering solid solutions where the end members may have established (but different) values of the on-site correction term.⁵⁰

The majority of compounds considered for both battery applications and solid oxide fuel cells are paramagnetic at their operating temperatures. However, as many DFT calculations are commonly based on energy minimisation, correctly identifying the lowest energy, zero temperature structure requires the correct magnetic ordering to reproduce accurate bond lengths and defect interactions. Neglecting spin polarisation for magnetic species that are diffusing (for example, transition metals in a non-magnetic host metal lattice^{51,52}) certainly leads to significant misrepresentation of the migration energies but it is unclear whether similar care is needed for non-magnetic ions, such as oxygen or lithium ions, in a host crystal which exhibits a fixed magnetic ordering in its ground state. Relatively small energy differences have been reported between magnetic states (0.01–0.1 eV/ion) compared with defect formation and migration energies (~ 1 eV)⁵³ but recent work has highlighted quite subtle effects on calculated migration pathways^{54–56} and these should be investigated.

The practical machinery of a solid-state DFT calculation normally consists of an iterative, self-consistent solution to the Schrödinger equation using a Hamiltonian which itself is a functional of the electron density (calculated in turn from a trial wavefunction). This can be used to predict the ground

state energy (or any ground state property) of a system of electrons to a specified energy tolerance. There are a number of pragmatic approximations, particularly in periodic systems, that may make these repeated calculations more efficient with minimal loss of accuracy: the truncation of the wavefunction in reciprocal space up to a certain finite value (the cutoff energy), the use of a combined pseudopotential representing the atomic nuclei and chemically inactive core electrons to remove rapidly varying, and therefore high energy, parts of this basis set,⁵⁷ and the discretisation of the electronic density over a grid of points in reciprocal space (the k -point grid or spacing).⁵⁸ All of these have a sound mathematical basis and are a judicious compromise between speed and computational accuracy especially when they allow the use of larger system sizes, more calculations, or more complex functionals. They may however affect the reproducibility, accuracy, or transferability of the results and we echo the advice of Mattsson and coworkers⁴⁴ in the importance of reporting these parameters in published work.

B. Empirical potentials

In spite of the mathematical paraphernalia required to approximate the solutions to the wave equations, the resultant energies and forces between atoms in crystals almost always tend towards the familiar ionic, covalent, or metallic bonds that we would recognise from general chemistry.^{59,60} These are often well described by much simpler expressions. The great advantage of these parameterised forms is that the energy can be expressed simply as a function of the atom positions (rather than a variational ground state energy obtained through DFT). Their evaluation is therefore several orders of magnitude quicker than electronic structure calculations. Since the inception of computer simulations of atomic motion,^{61–63} the use of parameterised or effective potentials has always led to true *ab initio* methods in terms of system size and accessible timescales.⁶⁴

These parameterized potentials describe the potential energy between atoms within the classical Born-like description of the crystal lattice.⁶⁵ The interactions between pairs of ions are partitioned into a short-range potential energy (for example, the Buckingham or Born-Mayer-Huggins potentials^{66–68}) together with a long-range Coulombic term. The imposition of a point electrical charge does not imply that the system is fully ionic⁶⁹ and in many cases, partial charges are used rather than the full valence charge of each ion. More complex potential forms have also been introduced^{70–74} which offer modifications to address some of the simplifications of the Born model through better consideration of many body dynamics. The fitted data for the parameterised potentials are traditionally based on the bulk thermophysical properties of the crystal (for example, the elastic constants or thermal expansivity) but increasingly these are being supplanted through high quality DFT calculations of point and extended defects.⁷⁵

C. Estimating diffusion from molecular dynamics (MD)

Either DFT or parameterised potentials may be used to predict the energy of a configuration of atoms. Static energy

calculations of these configurations may enable the study of some aspects of diffusion (for example, defect binding energies); however, ultimately dynamics are required in order to fully understand how to predict and optimise diffusion. We discuss first the most direct route of calculating diffusion through molecular dynamics (MD) simulations, which model a very small portion of matter at a specified external temperature and pressure in order to directly model the diffusion processes in the correct thermodynamic equilibrium. This is frequently employed with empirical potentials but a growing body of DFT calculations have been developed despite the considerable computational burden. Following this, we discuss how energy minimisation can provide insights of the dynamic behaviour of crystals which may be used to predict the diffusivity of a species without needing to perform long timescale simulations.

Molecular dynamics simulations establish how a given configuration evolves over time by numerical integration of Newton's laws. This is attractive as over a long period of time it allows all of the various configurations of a system to be sampled with their correct thermodynamic probability, and assuming that the underlying DFT or potentials are accurate, is probably the closest we may come to visualising atomic time and length scales. In practice, the rapid oscillations of atoms around their equilibrium sites (in the terahertz range) mean that MD requires very small integration time-steps of around a femtosecond to reproduce the system dynamics, even modest timescales therefore require the accumulation of very large numbers of iterations.

The system size of the computer simulations must contain sufficient atoms to model the crystal and its defects but also sufficient extra material to negate image-image interactions (assuming, as is common, a periodic system). This is particularly challenging for ceramics as the Coulomb interaction between pairs of charged defects decays much more slowly than other interaction terms. In the past, this has been a significant restriction of the applicability of molecular dynamics. The system size is, however, a parameter that adapts well to the parallelisation available on modern computing clusters. Current simulations using empirical potentials are able to model crystalline materials with billions of atoms, which with some judicious choice of boundary conditions, enable dislocations, boundaries, and even semi-realistic grain sizes to be studied. DFT-based molecular dynamics simulations are vastly more expensive but have recently been able to consider not just point defects in ceramics but the dynamics of their interaction with extended defects such as dislocations.⁷⁶ It is likely that the rapid pace of increasing computational power will extend the scope of simulations in the short and medium term.

Modelling long timescales, and in particular, the influence of rare events on diffusion, is a greater challenge.⁷⁷ Currently, traditional MD using parameterised potentials can routinely access nanosecond timescales for millions of particles. However, simulation time is sequential so larger computers only gift us the ability to reach the same nanosecond timescales for greater numbers of particles. Many simple diffusion processes are ergodic and so the spatially averaged behaviour of a configuration of atoms can provide a

substitute for a lack of knowledge of long time behaviour. There are still significant challenges however if we wish to model long time scale processes, such as the ageing of materials after many charge/discharge cycles, with atomic scale resolution.

Given that the simulation techniques are capturing the relevant atomic processes, how do we actually link these to experimental parameters, for example, the bulk diffusivity, D ? Assuming that we have an MD simulation of sufficient length of time to provide a statistically useful number of ion hops the most direct method is from a measure of the displacement of the mobile ions through the Einstein relationship:

$$D = \lim_{t \rightarrow \infty} \frac{1}{6t} \text{msd}(t), \quad (6)$$

where the mean squared displacement of the N mobile ions at a time t after a reference time t_0 is defined to be

$$\text{msd}(t) = \frac{1}{N} \sum_{i=1}^N |\vec{r}_i(t) - \vec{r}_i(t_0)|^2, \quad (7)$$

where $r_i(t)$ denotes the position of ion i at time t . If the simulation has covered a sufficient amount of time, then a plot of $\text{msd}(t)$ against time will be linear, and in the absence of infinite time, the asymptotic gradient of this plot will be a good approximation to the limit described in Eq. (6). A second, less frequently used, method of calculating diffusion from the velocity autocorrelation function⁷⁸ which recognises that the position of an atom can be written as the time integral of its instantaneous velocity (a per-atom property calculated during the MD simulation), and therefore the mean squared displacement in Eq. (7) may be evaluated by numerical integration of the autocorrelation of an atom's velocity vector over long times.

D. Estimating diffusion from molecular statics

The greater computational cost of DFT usually precludes its use in establishing diffusion coefficients through Eqs. (5) and (6). However, there are direct ways of accessing the activation energy provided the dominant point defects and their migration pathways are known, or can be reliably guessed. In particular, transition state optimisation using nudged elastic band^{79,80} or synchronous transit⁸¹ methods have been used extensively to establish the minimum energy required to move from one atomic configuration to another (i.e., the individual values of E_m in Fig. 1). From this it is possible to reconstruct the overall activation barrier for diffusion by stringing together each migration hop in order to form a continuous path. This is often all we need to discriminate between different candidate materials, as estimating the activation energy for diffusion [rather than the absolute value of diffusivity as given in Eq. (6)] frequently results in the optimum material selection given the importance of lower temperatures in commercial batteries and fuel cells.

The difficulty with transition state search methods is that they assume details of the diffusion pathway are known. In many simple structures, this may be obvious and the

contribution of higher energy migration pathways is inconsequential. However, there are examples where migration of defects occurs via non-intuitive pathways, for example, the ‘‘additional’’ site identified in oxygen migration in apatites⁸² or the interstitialcy mechanism proposed in $\text{La}_2\text{NiO}_{4+\delta}$.⁸³ The success of this transition state optimisation is therefore dependent on being able to identify *all* of the important diffusion pathways, not just a subset of them.

Various automated discovery methods have been proposed using the attractively simple MD approach whilst retaining the ability to examine long timescales. The most frequent technique is adaptive kinetic Monte Carlo, in which transition state calculations (using either DFT or empirical potentials) are coupled with a framework code that evolves a system according to a set of steps or atom hops that are calculated on-the-fly.^{77,84} By dispensing with the need to simulate the atoms vibrating around their equilibrium positions, and thereby concentrating on the actual migration process, these methods can achieve simulations of diffusion running into milliseconds of time whilst still retaining full atomic scale fidelity. We also highlight the success of accelerated- or hyper-dynamics methods developed by Voter and co-workers at Los Alamos National Laboratory.^{77,85,86} These attempt to address the timescale problem through recourse to transition state theory in order to directly accelerate molecular dynamics simulations. These may be useful in predicting the evolution of energy materials, for example, the long term segregation of species leading to electrode ageing, or the prediction of complex and rare defect clusters that may have a disproportionate effect on the overall migration rate.

Implicit within many reported DFT calculations and all empirical potential calculations of diffusion is a presumption of the dominant mobile species. In real crystals, the formation enthalpy and therefore concentration of the mobile defects will vary with the external chemical potential of the defect and the (temperature dependent) contribution of electronic and vibrational entropy and energy. This may lead to non-Arrhenius behaviour, which will not be captured through either migration or defect energy calculations, and even a switching of the dominant defect type in different temperature regimes.⁵⁵ Calculating accurate values of these various contributions within DFT is possible but complex even in relatively simple crystal structures: for example, recent work has offered a robust framework for defect enthalpies in metal-oxide systems.²⁶ Extending these calculations to more complex compounds is a non-trivial exercise requiring calculations that exhaustively consider plausible defect arrangements, are sufficiently accurate and reliable to provide quantities such as the phonon density of states, and also transferable such that the energy changes can be couched in absolute terms to external reference points such as a well characterised oxide or the ionisation of an O_2 molecule.^{87,88} Despite these difficulties, predictions have been made that show excellent agreement with experimental values of diffusivity across a wide range of temperatures and external conditions using solely static and transition state DFT calculations.^{26,55,89}

The choice of DFT or parameterised pair potentials is problem-specific. Pair potentials have a clear advantage in

the system size or timescales accessible, as a rough guide traditional DFT is a factor of around 10^5 times more computationally expensive per unit time or (each) linear dimension.⁶⁴ Empirical potentials, however, require a robust parameter set and will struggle when required to predict more chemically orientated behaviour, for example, charge transfer, mixed ionic and covalent bonding or interfaces between different classes of materials. DFT simulations of dynamic behaviour are still challenging and require either significant computing infrastructure to obtain the long timescale behaviour or a comprehensive understanding of the crystallography of a system in order to confidently identify all of the possible transition pathways and defect configurations.

IV. OXYGEN DIFFUSION MECHANISMS IN SOFCs

Considered here are two applications of materials in solid oxide fuel cells, the electrode and the cathode both of which have exacting property requirements and considerable commercial interest in improving their performance. The electrode is subject to large differences in chemical potential (pO_2 from 1 to 10^{-15} atm) due to the porosity of both the cathode and anode and therefore, it must be chemically stable across a wide range of oxidising and reducing conditions. It should also display close to pure ionic conductivity at the operating temperatures as any electronic conductivity will cause a partial short circuit and reduce the cell efficiency. Cathode materials are both electronic and ionic conductors and require high oxygen diffusion (and rapid surface exchange rates) in order to promote an extensive reaction volume with the supplied fuel. The materials chosen must also be chemically compatible with other elements of the cell, for example, avoiding the formation of insulating phases at the boundary,^{90,91} and have similar thermal expansion coefficients to avoid cracking and delamination at the interface during repeated heating and cooling cycles.^{8,92}

Recent developments in fuel cell infrastructure have placed a premium on materials that can achieve the combination of these properties at lower operating temperatures (500–700 °C) rather than the highest absolute oxygen diffusivity.¹³ These lower operating temperatures hasten the adoption of SOFCs through lower costs and reduced concerns over material degradation and ageing due to prolonged high temperature service. The commercial drive to reduce operating temperatures of fuel cells has focused the community's attention on producing materials that have low activation energies for oxygen diffusion, as these will preserve high levels of oxygen transport at low temperatures. Many oxides do have relatively low intrinsic migration energies due to the large and highly polarisable electronic structure of the oxygen ion; this permits a range of different chemistries and an easy passage through the surrounding ion sublattice. The difficulty is that oxides are generally intolerant of deviations from stoichiometry and the low migration energy is therefore often coupled with very low levels of intrinsic point defects. The challenge in oxide crystals is to introduce dopants which contribute charge-compensating oxygen-ion vacancies or interstitials but do not obstruct or hinder the migration route for bulk diffusion.

In this section, we focus on oxygen diffusion in doped ceria (CeO_2) which is an alternative solid-electrolyte with better low temperature performance than the more common cubic stabilized zirconia (CSZ). We then contrast this with the diffusion mechanism in cathode materials formed from perovskite and layered-perovskite Ruddlesden-Popper phases. These are an example of more complex crystal structures, with highly anisotropic migration pathways, compared to the relatively simple crystallography of ceria. Finally, we discuss the promising new work on oxygen ion diffusion in silicate and germanate based apatite phases.

A. Doped-ceria

Doped-ceria (CeO_2 with aliovalent dopants) is a fluorite-structured crystal, as illustrated in Fig. 2. It is gaining increasing use in intermediate temperature oxide fuel cells due to its high oxygen diffusivity, rapid oxidation and reduction kinetics, and chemical stability. At intermediate temperatures, it outperforms the more common and structurally related cubic-stabilized ZrO_2 (CSZ) despite its non-negligible levels of n -type electronic conductivity at temperatures above 600 °C. Practical fuel cell examples have demonstrated the use of the material with only a small resultant drop in voltage due to the parallel electronic component.⁹³

Even in the undoped case, the intrinsic oxygen diffusivity in ceria is substantial at high temperatures, as the normal Frenkel pair concentration of defects is swollen by oxygen vacancies produced through the reduction of Ce^{4+} ions to Ce^{3+} charge states.⁹⁴ The mobility of these oxygen vacancies has been modelled using DFT^{27,95} and in this simplest case has revealed a cooperative hopping of individual oxygen vacancies accompanied by a dynamic redistribution of electronic charge across cations during the migration process.⁹⁶

The benefits of ceria electrolytes are more compelling at low temperatures and the majority of studies have therefore

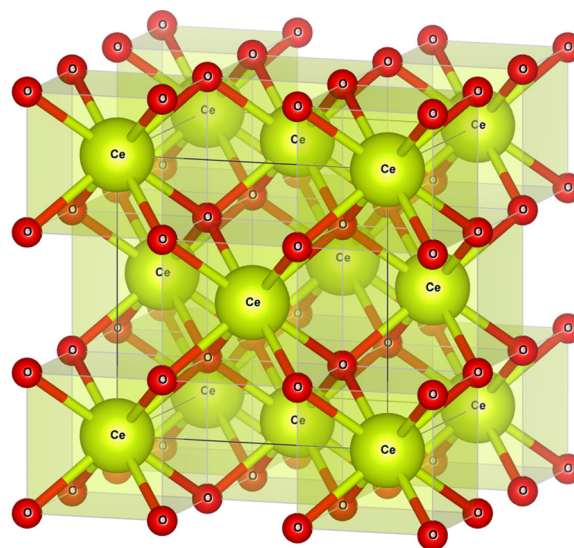


FIG. 2. Crystal structure of CeO_2 showing the cubic unitcell (black lines) with Ce and O atoms in yellow and red, respectively. Trivalent metal ion substitutions take place on the Ce sites with accompanying oxygen vacancies on the oxygen sites.

examined the behaviour of ceria when doped with aliovalent metal ions to preserve the low temperature diffusivity. The mechanism of improved oxygen diffusivity through doping CeO₂ (and similarly in ZrO₂) occurs through the formation of charge compensating oxygen vacancies. For example, the reaction of a rare earth oxide, Re₂O₃, with ceria



where the rare earth cation substitutes directly onto the Ce site and the oxygen hypostoichiometry is accommodated through the formation of doubly charged oxygen vacancies within the host lattice.⁹⁷

In principle, many trivalent cations will provide compensating oxygen vacancies and indeed the range of soluble rare earth elements into CeO₂ is extensive. In practice, the link between dopant species, concentration, and bulk oxygen diffusivity is not a simple relationship and becomes more complex when we consider multiple substitutions of either alio- or isovalent (e.g., Zr_{Ce}[×]) cations. Atomic scale simulations have therefore been able to provide guidance as to which dopant, or combination of dopants, should provide the lowest activation energy for bulk oxygen diffusion.

Several authors have looked at the effect of single, dilute ion species on the oxygen migration barriers and all remark on the additional complexity this creates. For example, the introduction of an isolated Pr_{Ce}['] defect alters the migration barriers surrounding the ion to a range between 0.41 and 0.78 eV,⁹⁵ but it also traps the oppositely charged oxygen vacancies near to the substitutional metal site. The trapping distance is a competition between the Coulombic attraction and the requirement for the local strains to be accommodated in the lattice; for Pr-doped ceria this occurs at the second-nearest neighbour site but Gd_{Ce}['] defects (for example) prefer a first nearest neighbour oxygen vacancy.⁹⁸ These results highlight the requirement to consider not just migration barriers, or the increase in charge carrier concentration, but the entire pathway required for bulk diffusion.

The effect on migration barriers and different levels of binding have led several authors to consider the question of which ions promote the highest overall diffusivity.^{99–102} The consensus that has emerged is this is driven by the substitutional ion size, for example, in the lanthanide series ions with a smaller radius (or a greater atomic number, *Z*) than _{*Z*=61}Pm tend to nearest neighbour coordination with oxygen vacancies and ions with radii greater than ₆₁Pm tending to a second nearest-neighbour. Andersson *et al.*⁹⁹ categorise this behaviour in terms of the competition between the interaction between strain fields (driven by the size of the trivalent ion) and the attraction between oppositely charged point defects. Using configuration averaging of the different cation positions they arrive at an overall activation energy for diffusion which is lowest for ₆₁Pm or ₆₂Sm dopants. Pm is radioactive and unlikely to be commercially used, however the high diffusivity of Sm-doped ceria has been confirmed.¹⁰³ Recent experiments based on comparison of similar prepared samples with different rare earth dopants has however revealed that there are still some puzzling features of the

diffusion behaviour, in particular, the link between low levels of elastic strain and optimum diffusivity.¹⁰⁴

As well as the dopant species, there is also a non-linear relationship between the dopant concentration and the oxygen ion diffusivity in doped-ceria. At low dopant levels, the diffusivity rises with the dopant concentration as a greater population of charge carriers is produced. This increase, however, does not scale simply with dopant concentration and may eventually start to decline, for example, in Gd- or Sm-doped ceria conductivity is reported to drop as levels are increased beyond about 10 wt. %.^{105,106} Experimental measurements of this change as a function of dopant species and dopant level have revealed a pronounced drop and then subsequent rise in activation energy for electrical conduction.¹⁰⁷

This non-intuitive result was considered in early modelling work which identified the importance of oxygen vacancy ordering and clustering around substitutional metal ions;^{108,109} in particular, at low dopant levels, oxygen ion vacancies are generally bound to individual metal ion dopants and long scale diffusion depends on them bridging between these point defects. Higher dopant levels lead to a frustration of the oxygen ion mobility due to the organisation of oxygen vacancies into small clusters^{110–112} and a forced transition between a preference for next nearest neighbour to nearest neighbour coordination.^{113,114} Co-doping with multiple trivalent ions dramatically increases the number of possible configurations; however, initial studies have shown that it is an effective method to suppress the formation of larger, immobile oxygen vacancy clusters and therefore improve diffusivity at higher dopant levels.^{115,116}

The importance of the strain fields surrounding point defects in determining the optimum level of diffusivity leads us towards a second method of controlling diffusivity in ceria. This is through the deliberate introduction of strain into the equilibrium host lattice through doping with isovalent foreign ions, for example, Zr_{Ce}[×], or layered heterostructures which result in extended epitaxial strain fields at the interface between different compositions.^{117–120} The effect of imposed lattice strain has been noted for several years;^{117,121} however, recent interest has been sparked by reports of a dramatic eight order-of-magnitude increase in conductivity in epitaxially grown zirconia-strontium titanate heterostructures.¹²² Although the magnitude of the change is not without controversy,¹²³ many other studies have also made a clear link between imposed lattice strain and an increase in the oxygen diffusivity in CeO₂,^{124,125} ZrO₂, and other fluorite structured oxides.¹²⁶

The role of strain in altering ionic conductivity has generated several atomic scale studies in order to confirm the effect, examine its possible magnitude, and search for a possible origin. Strain is well defined on an atomic scale and easy to modify in simulations and therefore, most authors have looked at the direct effect of compression or expansion of the cell axes on the net diffusivity or migration energies.^{124,125} These studies support an effect of strain in both the doped and undoped cases. The origin of the effect is at least partially attributed to the changes in the vacancy to rare-earth binding energy;¹²⁴ however, the observation of the

effect in the undoped case also suggests a more fundamental relationship between lattice strain and the activation energy.

Although absolute levels of diffusivity have been the main driver for improving ceria based electrolytes, several studies have also considered a more nuanced approach in considering both the thermal stability, compatibility with other substrates, and device ageing. For example, the experimental work of Hong and Virkar⁹⁷ was recently analysed and developed by Marrocchelli and co-workers to provide a general approach to modelling and predicting chemical expansivity within doped ceria systems.³⁰ These results are important both in understanding the potential incompatibility of different dopant containing materials but also in designing new materials with combinations of dopants that lead to near-zero chemical expansion.

Doped ceria is structurally the simplest compound considered in this review. We pause at this point therefore to consider the contributions atomic scale simulations have made to our understanding of the dynamics of the diffusion process:

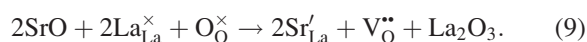
1. Oxygen diffusion in doped ceria is achieved through a vacancy diffusion mechanism; however, the influence of dopant ions on this diffusivity is not simple. Atomic scale simulations have been used to isolate the various contributions due to elastic strain effects and Coulomb interactions.⁹⁹ This opens the way to developing predictive design rules based on the ionic size to optimise the choice of dopant ions.
2. Dopant ion concentration determines the net concentration of oxygen vacancies and therefore the availability of charge carriers, but this is not a linear relationship. It is frustrated at higher dopant levels by vacancy-vacancy interactions and the formation of less-mobile oxygen vacancy clusters around foreign cations. Kinetic Monte Carlo models have shown an ability to replicate these effects^{84,112} and are likely to be the only currently available method of optimising the composition of materials with significant dopant levels and multiple cation substitutions.
3. The effect of lattice strain on diffusivity, as imposed by layered heterostructures, is difficult to study experimentally as measurements are often done on bulk properties and may be conflated with the effects of electronic conductivity.^{122,123} The use of atomic scale simulations supports the effect of strain on oxygen ion diffusivity in doped ceria and offers a clear way to study and potentially optimise the effect through either isovalent dopants or tailored microstructures.

It is also important to stress that even in this simplest material, the questions being asked are beyond the capability of chemical synthesis to explore all possible compositions. And the non-linearity of diffusivity with dopant concentration and strain means that finding the best composition cannot proceed via a simple serial search. Understanding the diffusion process on an atomic scale is the only method capable of predicting optimum diffusivity simultaneously across many different compositions.

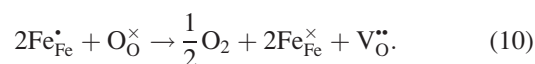
B. Perovskites

Perovskites are oxide crystal structures with the general composition ABO_3 where A is often a rare earth or alkali metal and B is often a transition metal. They display an approximately cubic structure consisting of the larger A ion surrounded by eight, corner-sharing BO_6 octahedra as illustrated in Fig. 3(a). The ability of the octahedra to tilt and twist give the A and B sites the ability to adapt to a wide range of different cations, and combined with the polarizability of the oxygen ions, perovskites exhibit a broad range of material properties arising from the strong coupling between their crystal structure, the electronic structure, and their magnetic structure.¹²⁷

Ionic conductivity in perovskite structured oxides was first identified in $LaGaO_3$ by Ishihara and co-workers¹²⁸ who determined that Mg and Sr cation substitution produced the highest overall oxygen self-diffusion through the formation of mobile oxygen vacancies (rather than electron holes at lower temperatures¹²⁹) through the reaction



Most SOFC-relevant perovskites consist of rare-earth or alkaline metal ions on the A -site (e.g., La and Sr or Ca and Ba) and a mixture of reducible, transition-metal ions on the B -site (e.g., Mn, Ni, Fe or Co). The concentration of oxygen vacancies is determined by Eq. (9) but additional vacancies, prevalent at high temperature or low oxygen partial pressures, may also be formed by reduction of the B -site cation, for example, the reduction of Fe^{4+} to Fe^{3+} produced doubly charged oxygen vacancies through



Maximising the oxygen diffusivity in these materials requires low values of the overall migration energy (including trapping by aliovalent dopants³¹) and formation energy of oxygen vacancies [using both Eqs. (9) and (10)]. This

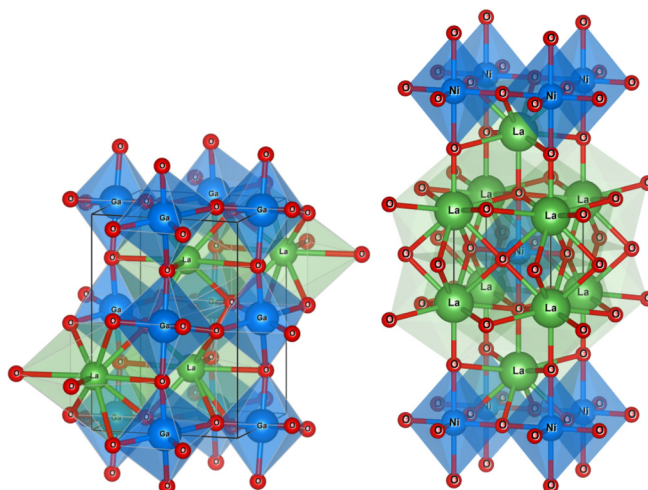


FIG. 3. Plots Showing (a) the perovskite structured $LaGaO_3$ and (b) Ruddlesden-Popper phase La_2NiO_4 ; the Ruddlesden-Popper phase is built up of alternate perovskite layers interspersed with rocksalt LaO layers.

must also be balanced against the overall stability of the perovskite lattice and the tendency of high concentrations of oxygen vacancies to form ordered arrays in Brownmillerite-type phases with a consequent fall in oxygen mobility.^{129–131}

The initial observation of the high levels of ionic conductivity in doped-LaGaO₃ perovskites was first examined using atomic scale simulations based on empirical potentials. These identified the lowest energy diffusion pathway,¹³² which consists of a curved migration of an oxygen vacancy in an arc around the GaO₆ octahedra and also show good agreement with experimental values of the migration energy.¹³³ Further powder diffraction work confirmed this prediction through maximum entropy refinement of diffuse neutron scattering data.¹³⁴ The role of the isovalent Mg codopant was also examined and found to control the tilting of the GaO₆ octahedra with higher levels of oxygen diffusion being attributed to the higher symmetry structure.¹³⁵

Atomic scale simulations have been used to identify the role of each possible dopant, in particular, the role of cation trapping of charged defects.^{132,136} Sr substitution was found to have a surprisingly minor effect on binding to oxygen vacancies; however, Mg ions were proposed to have a dual role in stabilising the GaO₆ octahedra and increasing the solubility of Sr¹³⁷ but also increasing the overall activation energy for migration.¹³⁸ The formation of Mg-V_O clusters predicted by simulations has also been mooted as an explanation for the distinct non-Arrhenius behaviour reported for LaGaO₃-based compounds.¹³⁹ A number of empirical potential studies have also considered doping on the *B* site to form LaBO₃ (*B* = Cr, Mn, Fe, Co).^{133,140,141} Again these show good agreement with experimentally determined structures and trends.

One important issue highlighted by the empirical potential studies is the failure in some cases to fully account for the variation in oxygen vacancy concentration as a function of temperature, chemical potential, and cation dopant. The diffusivity is constructed from both the migration energy and the concentration of mobile defects [Eq. (5)], and as the latter may change dramatically with temperature and oxygen partial pressure,¹⁴² then this will be reflected in the overall activation energy but not in the migration energies calculated from atomic scale simulations. There has been a sustained effort to use DFT to address this problem and to predict the oxygen vacancy concentration (and therefore diffusivity) for a specific, chosen composition from first principles. These calculations require absolute values of energy related to some well-characterised external reference state, often an oxide^{87,143} as the O₂ molecule is poorly predicted by traditional LDA and GGA (although hybrid functionals appear to fare better⁴⁹). Doping with transition metals on the *B* site also requires the use of hybrid functionals or the Hubbard correction in order to capture the correct electronic structure, although in the latter case the absence of band gap measurements for many of the solid solutions, or in some cases the end-members, has proven problematic.⁵⁰ There are also significant effects of vibrational entropy [contributing as much as 0.5 eV to the vacancy formation enthalpy at 1000 K in La_{0.5}Sr_{0.5}Co_{0.25}Fe_{0.75}O₃ (Ref. 144)] Despite these challenges, several recent publications have shown significant

progress not just in understanding the complex defect chemistry in perovskites but as a fully predictive model. We note as examples the complex role of Sr in vacancy formation enthalpies,^{89,144} the prediction of the quasibinary phase diagrams for the BaFeO₃-BaCoO₃-SrFeO₃-SrCoO₃ system,⁵⁰ and the use of DFT to examine SmCoO₃, a promising but relatively uncharacterized material for SOFC cathodes.¹⁴⁵

The perovskites are a system that allows a direct comparison of the use of empirical potentials and electronic structure methods. Many recent studies have defaulted to DFT because of the complex, multiple cation substitutions and that DFT is required to assess many of the other important properties of perovskites such as their optical and magnetic properties. Correctly predicting the charge state and energies of defects and their relation to the band structure of the material is better performed using electronic structure calculations,¹⁴⁶ and as discussed, the concentration of oxygen vacancies as a function of temperature and oxygen partial pressure is only really captured through the use of DFT. However, careful derivation and application of empirical potentials, often including cations with multiple possible charge states, can still yield valid results for basic defect chemistry and migration pathways and also the ability to consider large defect clusters which may be important in net migration values. The study of Mather and co-workers, for example, considered oxygen vacancy-cation dopant complexes up to two vacancies and four cations¹³¹ in doped CaTiO₃ with a range of substitutions and size of simulations. A feat that would likely be beyond the current capability of DFT. The choice between empirical potentials and the (inarguably) more complete description of DFT may depend on the influence of larger defect complexes on the overall migration process.

C. Layered perovskites

The ability of perovskites to adapt their structure is not limited to point defects, and several classes of materials have been synthesised that are based on crystals formed from multiple layers of perovskite and other common oxide structures. Of particular interest to the fuel cell community has been the Ruddlesden-Popper series of layered oxides in their use as mixed ionic/electronic conductors for cathode materials.^{147–149} Although not in widespread commercial use compared to the parent perovskite phases, they possess a low activation energy for oxygen transport which underpins their intended use at intermediate operating temperatures. They also offer the possibility to mitigate against some of the problems of traditional perovskite cathode materials, specifically better chemical compatibility with common electrode materials⁹¹ and improved thermal stability.^{92,150}

The first members of the Ruddlesden-Popper series, with general formula K₂NiO₄, consist of alternating layers of perovskite (KNiO₃)⁻ and rocksalt (KO)⁺ structural motifs. The parent, high-temperature structure of these is tetragonal (space group I4/mmm) and is illustrated in Fig. 3(b). The Ruddlesden-Popper structure shows a high degree of compositional flexibility which manifests both through a tolerance of significant oxygen hypo- or hyper-stoichiometry and the

accommodation of a diverse range of metal ions on the cation sub-lattice. Although the impact of cation substitutions on the structure is subtle, they can significantly alter the diffusion and surface reaction rates of the materials. For example, the intermediate-temperature oxygen ion diffusivity in $\text{La}_2\text{NiO}_{4+\delta}$, one of the first members of the series to be proposed as a cathode material,¹⁵¹ is significantly poorer than $\text{Pr}_2\text{NiO}_{4+\delta}$, despite the apparent similarities of the crystal structures.¹⁴⁸

In order to improve the performance of devices based on these materials, it is necessary to understand the diffusion process. Atomic scale simulations have been used in supporting this understanding for two reasons: they allow direct prediction of diffusivity and activation energies allowing a wide range of compounds to be examined and they also provide a mechanism of using the atomic scale motion to predict time- and spatially averaged data such as that obtained from x-ray or neutron diffraction analysis.

The first series of atomic scale simulations to consider these compounds used classical pair potentials to predict the structure and diffusion at a variety of temperatures and with a range of different metal ions.^{83,152,153} Figure 4 illustrates the overall structure and diffusion mechanism including the time averaged cation positions and oxygen ion density distribution [Fig. 4(a)], the oxygen density distribution projected in the plane of the oxygen apical sites [Fig. 4(b)], and plots showing the progress of the oxygen interstitial during its migration process [Fig. 4(c)]. In addition, these simulations

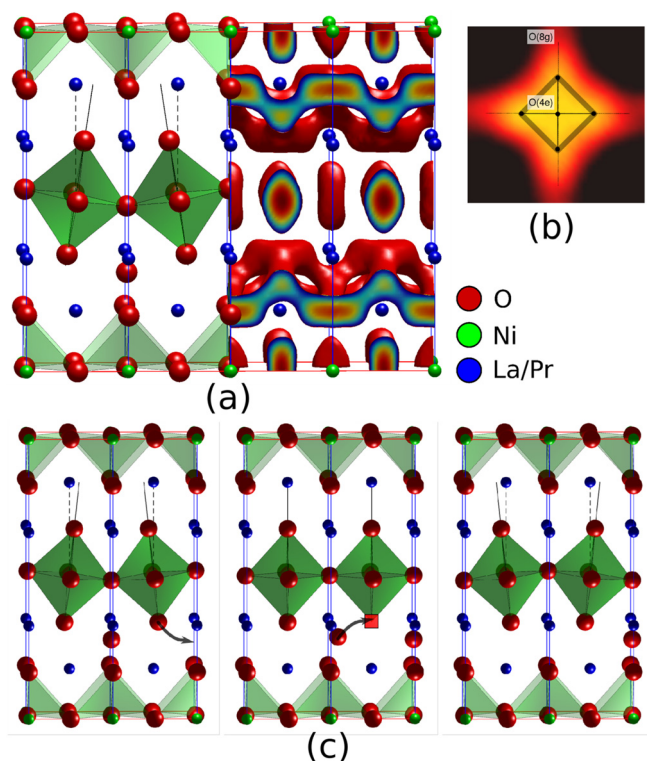


FIG. 4. Details of the oxygen ion diffusion mechanism in $\text{K}_2\text{NiO}_{4+\delta}$ ($K = \text{La, Pr}$) showing the (a) overall crystal structure including the time and spatially averaged oxygen ion isosurface; (b) a contour plot of average oxygen ion density through a unitcell at the $z \approx 1/4$ plane and (c) the interstitial mechanism responsible for oxygen ion diffusion in the dilute limit ($\delta \rightarrow 0$). Reproduced with permission from Parfitt *et al.*, Phys. Chem. Chem. Phys. 12, 6834 (2010).¹⁵³ Copyright 2010 Royal Society of Chemistry.

replicated both the absolute value and activation energy for oxygen ion self-diffusion and the structure of the material as established through maximum entropy refinement of neutron diffraction data.¹⁵⁴ The agreement of such simple pair potential models with both the structural and dynamics of the crystal is perhaps surprising, but further DFT studies of this and related materials suggest that, although there is evidence of magnetic ordering and charge transfer within these structures, the overall impact on the oxygen ion migration pathway is relatively inconsequential.^{155,156}

The complexity of the Ruddlesden-Popper crystal structure including the effect of magnetic ordering does mean that each convergence cycle in DFT is computationally expensive. Currently, it has not been possible for researchers to replicate the long timescale simulations necessary to establish directly the diffusivity and activation energy of these materials at realistic temperatures. However, using the knowledge gained from the classical pair potentials and the neutron diffraction data, Perrichon and co-workers used a newly developed technique based on positional recurrence maps¹⁵⁷ to examine the effect of temperature and dopant ions on the predicted level of oxygen ion diffusivity.¹⁵⁶ These results are noteworthy, both because of their importance in understanding the mechanism of coordinated mobility in these materials and also in the combination of better crystallographic understanding and carefully selected DFT simulations in efficiently predicting long timescale diffusion without the need to run molecular dynamics to these timescales.

The use of atomic scale simulations for these materials has therefore been crucial in identifying the dominant diffusion mechanism, which is an important first step in optimising the conductivity, and also assessing the role of various different cations within the structure in altering this conductivity. Of particular note is the close link between the time-averaged structures obtained from MD simulations and that predicted from fitting to diffuse scattering data from neutron diffraction measurements.^{83,154,158} This combined use of the two techniques adds additional details to the diffraction data and validation to the modelling. We will return to this point in Sec. IVD on apatite materials.

Despite the recent activity in both experimental and modelling work, there are several outstanding questions from the work performed on Ruddlesden-Popper phases: there is no mechanism for oxygen ion diffusion along the c -axis, despite experimental reports of significant (though lower) conductivity along this direction in single crystals. There is also no definitive answer to whether diffusivity in hyperstoichiometric $\text{La}_2\text{NiO}_{4+\delta}$ is ultimately limited by a partial ordering of the oxygen interstitials due to their Coulomb repulsion or the presence of increasing numbers of oxygen interstitials causes a “stiffening” of the lattice leading to higher average migration barriers. Identifying which (if any) of these processes occurs, and is important, is a crucial step in realising the potential of these materials.

D. Apatite-based materials

Apatite-based oxygen ion conductors are a relatively recent addition to the family of materials used for SOFCs but

have already generated significant interest due to their exceptionally high values of diffusivity and the promise of further improvements. These synthesized compounds are crystallographically similar to the apatite minerals and biomaterials often studied in the fields of geology and biology. Significant oxygen ion diffusivity was first reported in silicate based apatites,¹⁵⁹ and later extended to germanium containing materials.

The general formula of the compounds of interest is $M_{9.33+x}(XO_4)_6O_{2+3x/2}$, where M is a rare-earth element and $X = \text{Si}$ or Ge . Structurally, the compounds are composed of monolithic XO_4 tetrahedra arranged in strings along the c -axis, with the remaining oxygen and metal ions occupying channels interspersed within. The resultant structure, shown in Fig. 5, is highly anisotropic both in terms of its physical properties and ion diffusivity.

The majority of SOFC related apatite materials are based on La accommodation on the metal ion site; this is driven by the observation that the largest ions ($M = \text{La}$, Pr , Nd) from the range of soluble lanthanides produce the highest ionic conductivity.^{159,160} A range of other minor dopants may also then be used across the M and X sites, with some ions (for example, Co) having the curious ability to substitute on to either of these crystallographically quite distinct sites.³² The tolerance of the structure to very disparate chemical substitution can be linked to the ability of the XO_4 tetrahedra, which form the structural backbone, to tilt and twist allowing both significant expansion and contraction around metal ion sites and even complete changes in the coordination number as seen for the very smallest metal ions (for example, Mg) on the La sites.¹⁶¹

As was seen in the example of the Ruddlesden-Popper phases, these complex structures often have ionic densities that are not well captured by the site-specific thermal ellipsoid and partial occupancy parameters that would be refined during Rietveld analysis of powder diffraction data. For example, the first published structures identified a band of highly anisotropic oxygen sites along the c -axis,¹⁶² which it is natural to conclude, are the pathway for oxygen diffusion. However, atomic scale simulations comparing $\text{La}_{9.33}(\text{SiO}_4)_6\text{O}_2$ and the

isostructural but poorly conducting compound $\text{La}_8\text{Sr}_2(\text{SiO}_4)_6\text{O}_2$ identified a further interstitial site which enabled a lower-energy migration pathway^{82,163} for the former, whereas diffusion in the latter occurred via a vacancy-assisted migration pathway. The importance of this additional interstitial site in controlling ionic diffusion was subsequently confirmed with additional powder diffraction structural refinement¹⁶⁴ and NMR data.¹⁶⁵

Further investigation of the local structure of the SiO_4 and GeO_4 tetrahedra may also help explain some of the puzzling features of the diffusion in these materials; in particular, the level of oxygen migration in the a - b plane is higher than might be expected from the anisotropy in the structure. This together with the comparable activation energies for diffusion from single crystal studies points to a further series of migration pathways operating between adjacent channels. Identifying these channels however is a significant challenge because their existence may be only transient due to favourable alignment of the SiO_4 or GeO_4 tetrahedra. Study of these dynamic pathways, similar in many ways to the percolation or paddle-wheel mechanism identified in superionic Li_2SO_4 and Na_2SO_4 crystals,^{38,166–168} is only accessible through atomic simulation.

E. Concluding remarks

Before leaving the topic of oxygen ion conductors, we reflect on the success or difficulties encountered in the use of the various techniques. For the examples considered here, empirical potentials have provided the first insight into the diffusion process and the effect of different dopant ions. DFT calculations however have been used extensively (and successfully) to model diffusion in doped ceria, and there are considerable advantages in this approach particularly in the flexibility to include many diverse ion substitutions without having to derive new potential parameters. We do see however some of the difficulties inherent in the DFT approach when applied to perovskite and perovskite-based materials. A greater number of ions are required to model these crystals

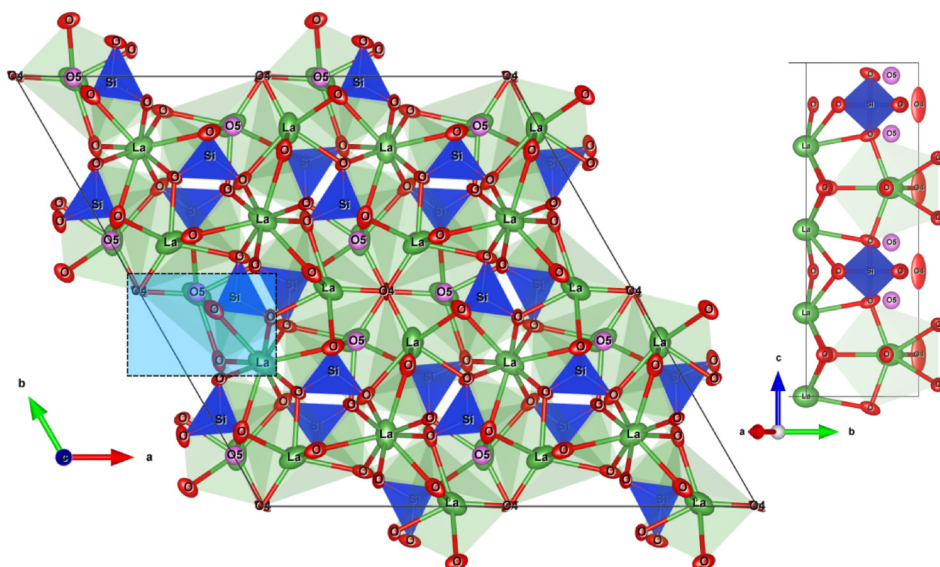


FIG. 5. Diagram of the parent apatite structure showing a $2 \times 2 \times 1$ supercell with the MO_4 tetrahedra in blue, metal M ions in green, and the central oxygen ion channel in red. The inset shows details of the highlighted atoms (blue box) viewed along the $b \times c$ direction. The O4 sites are partially occupied with highly anisotropic thermal ellipsoids with the major axis aligned along the c -axis; however, diffusion actually takes place via an interstitial site (O5) which has a very small occupancy as predicted from atomic scale simulations and later confirmed using powder diffraction Rietveld refinement.

because the unitcell is physically larger and the accommodation of long range elastic relaxation (for example, the tilting of the NiO_6 octahedra in Fig. 4) necessitates large supercells. It is also not trivial to assess in these larger, anisotropic crystals the coupling effect between a charged defect (e.g., an oxygen interstitial) and the actual zero stress cell parameters.^{169,170} It is likely therefore that in spite of the attractive simplicity of direct DFT MD simulations, there will still be a role for both empirical potential and targeted DFT simulations in studying these materials.

V. LITHIUM DIFFUSION MECHANISMS IN BATTERIES

Battery technology is fundamental to the current and future energy infrastructure as it offers methods to store energy, when generated at local or a grid level, and transport energy when separated from the grid, for example, in consumer electronics. The components of modern battery cells contain a cathode and an anode separated by an electronically insulating solid electrolyte,¹⁷¹ in common with the SOFC cells discussed previously, however there are important differences: the operating temperatures are lower and the diffusing ion is required to be stored alternately and repeatedly within the cathode and anodes during charge and discharge cycles rather than either acting as a reaction site for input of the fuel or removal of the exhaust. The materials chosen for the cathode for example are not only required to enable rapid ionic diffusion but must in addition provide a suitable reaction energy in order to maintain a sufficient open cell voltage for the battery.

The commercial drive to improve battery technology has settled on Li-ion materials as the primary system, and the low weight of Li means it is likely to remain as the lead system for applications where specific energy density is the central requirement. However, the recent interests in grid level storage where cost and reliability are preferred over raw energy density have led to interest in sodium based systems;¹⁷² sodium has significantly greater abundance and lower production costs. We stress that although the materials may differ between these two systems the techniques and approaches from atomic scale simulations are equally applicable to both.

Reaction energies at the cathode are one of the main drivers for improving battery performance as the gravimetric capacity of the most common graphite anodes typically exceeds the cathode due to the light weight of carbon.^{173,174} We discuss reaction energies here only in passing, however, as the individual energies are not directly related to diffusion within the materials. Nonetheless, we note that atomic scale studies are valuable in ascertaining these reaction energies for a wide range of compositions, and much like the case of diffusion, may provide the only method capable of accurately sampling all of the possible combinations for a given material crystallography.¹⁷⁵ The diffusivity of cations within the cathode and electrode determines the maximum charging and discharging rates (i.e., the power density) and also influences the tolerance of the cell to repeated charging cycles. Shorter charge cycles are desirable and the ability to reversibly accept and donate charged ions in a material is

important to the longevity of a cathode-electrode-anode coupling, and this behaviour has been systematically investigated using atomic scale methods.¹⁷⁶

In this section of the review, we will focus on the modelling of two leading cathode materials: the layered series of rocksalt-derived compounds similar to LiCoO_2 which exhibit two-dimensional diffusion and the olivine-structured phosphate-based materials which have one-dimensional diffusion pathways. Broadly, the rocksalt structured layered-compounds tend to find use where the highest energy densities are required and the olivine-structured phosphates where charge and discharge rates are most important. We will also discuss some interesting new results for high-conductivity electrode materials based on lithium lanthanum titanate and MXene compounds which show significant promise as lithium ion conductors.

A. Li_xCoO_2 and related compounds

Some of the first commercially successful solid-state cathode materials were lithium ceramics based on Li_xCoO_2 ,^{177,178} a layered crystal with general formula ABO_2 , where A is an alkali metal ion and B is a trivalent transition metal, most frequently described as an analogue of the α - NaFeO_2 structure.¹⁷⁹ In this crystal, a cubic close packed array of oxygen ions, illustrated in Fig. 6, forms octahedral cages for the two species of metal ions A and B which occur in alternate layers through the structure. The stronger, more covalent B -O bond provides the basis for the structure and permits considerable deviations from stoichiometry in the more weakly bonded AO_6 layers. This is accommodated through the reduction of the transition metal ion to provide charge compensation (for example, $\text{Co}^{3+} \rightarrow \text{Co}^{4+}$) for variable levels of Li-ion incorporation.

The high cost of Co, potential toxicity, and poor thermal stability of the compound¹⁸⁰ have led researchers to explore suitable alternatives based on similar structures. The requirement of variable valence states and compatible electronic orbitals has selected primarily Ni and Mn substitution onto the transition metal sites. These compounds are often prone to loss of capacity after charge cycling, due to the transformation of the layered structure into a defective spinel,¹⁸¹ but if this can be controlled, they offer a greater range of suitable chemistries.

These materials have been exploited to produce a range of Li and Na based cathodes which permit inclusion and then subsequent removal of the alkali cation from the structure. Although powder x-ray diffraction studies combined with arguments based on geometric factors and ionic radii provided an accurate description of the structure of the material¹⁸² and also a good approximation to the migration pathway,¹⁷⁹ detailed calculations of the complex crystallography that determine the overall diffusivity were only possible through atomic scale simulations. Initial work focused on Li_xCoO_2 , which was one of the first high activity compounds to be identified and put into commercial service. It exhibits large deviations from stoichiometry, with $0.1 < x < 1.0$ although this is accompanied by phase transformations and the coexistence of different phases;¹⁸² a practical

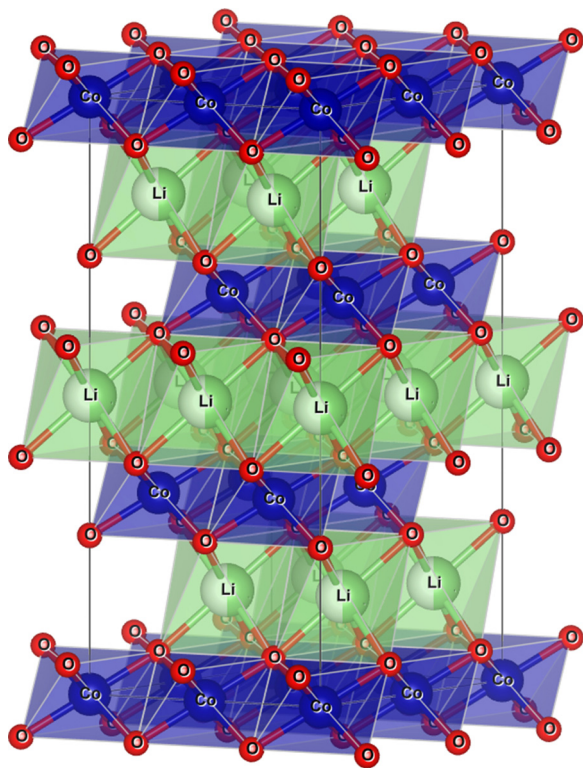


FIG. 6. Crystal structure of Li_xCoO_2 showing Li and Co and O ions in green, blue, and red, respectively. Li ion sites are able to tolerate substantial partial occupancy and cation disorder (exchange of the Li and Co ions) is also extensively observed.

operating range for commercial cells is from around $x = 0.4$ upwards.

One of the early observations in the use of these materials was the influence of cation disorder on the diffusion mechanism. For example, ball milling of Li_xCoO_2 samples dramatically reduces the capacity of the material.¹⁸³ This disordering, which is due to the replacement of Li with transition metal ions from adjacent layers, also occurs during charging and discharge cycles and therefore understanding and limiting its effect on the migration process is important in producing long lifetime cathode materials.

Early DFT calculations examined various transition metal substitutions on the Co site and identified the importance of the electronic structure in determining the ability of the compounds to maintain significant Li diffusion following the disorder driven through several charge/discharge cycles.¹⁸⁴ A key link was made between the bulk Li-diffusion, the transition metal species,¹⁸⁴ and the crystallographic layer spacing along the c -axis.¹⁸⁵ Larger spacing was associated with a greater physical separation between the transition metal cation and the Li ion during its transient passage through the tetrahedral site. Disorder of the structure causes a progressive reduction in the lattice parameter and a consequential increase in the activation energy¹⁸⁵ due to the requirement for the Li ion to encroach upon the transition metal site; loss of Li from the structure, which is crucial for high charging capacity also reduces the lattice parameter with again a significant reduction in diffusivity.¹⁸⁶

We may conclude from these arguments that disordered structures have a detrimental effect upon bulk diffusivity. However, careful design of the chemistry of these materials

led by DFT simulations has opened up a new range of compositions which are disordered but have demonstrated high levels of diffusion combined with good tolerance to repeated charging and discharging. For example, Lee *et al.*²⁰ examined the effect of multiple transition metal species within the structure and using simulations determined that $\text{Li}_{1.211}\text{Mo}_{0.467}\text{Cr}_{0.3}\text{O}_2$ (LMCO) as a promising new composition. The diffusion mechanism involves the Li-ion hopping through different octahedral sites by passing through one tetrahedral site (o-t-o) first²⁰ as illustrated in Fig. 7(a). The ease of migration is based on the arrangement of transition metal (TM) ions around the Li-ion; Figs. 7(b)–7(d) present the three different possibilities in a fully disordered arrangement of cations. The Li migration energy is driven by the electrostatic repulsion between Li ions and the local TM ions and therefore, the local number (0, 1, or 2) of the TM ions has progressively increasing migration energies. The key therefore to maintaining high levels of Li-ion diffusion is ensuring that in these disordered structures there are sufficient numbers of 0-TM sites to form a continuous percolation network through the structure. Importantly, even if the 1-TM channels become partially inactive due to disorder, a significant percentage of Li ions will be still able to circulate through the 0-TM percolating network.

Interesting points for future work would be the creation of a percolating network in other Li-TM disordered oxides. Lee *et al.*²⁰ supports this suggestion via two basic reasons. First, the regions around the 0-TM channel spot are only surrounded by Li sites; therefore, the TM contribution tends to be limited by the activation energy of Li diffusion. Second, it is established that the tetrahedron height for most of the disordered rocksalts is considered as the most appropriate for

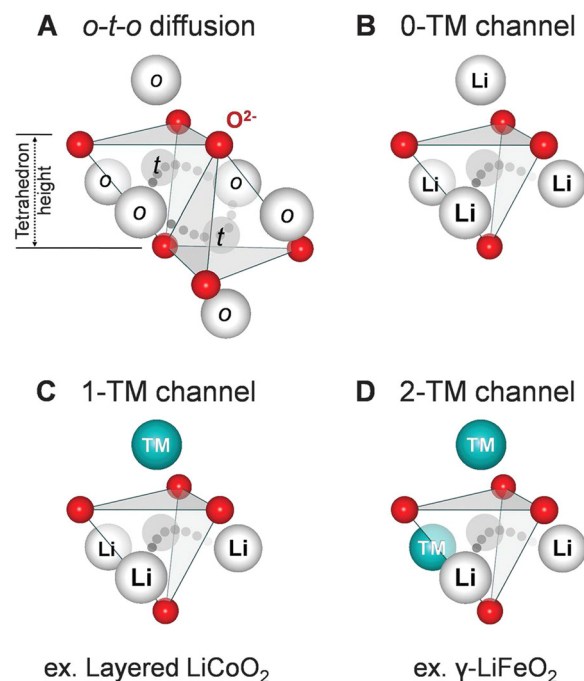


FIG. 7. Li-ion o-t-o hop possible environments: (a) Two tetrahedrons connected with a neighbouring octahedral. (b) Activated states share faces with no octahedral TM. (c) Activated states share faces with 1 octahedral TM. (d) Activated states share faces with 2 octahedral TM. Reproduced with permission from Lee *et al.*, *Science* **343**, 519 (2014).²⁰ Copyright 2014 Highwire Press American Association for the Advancement of Science.

those channels to be activated. Assuming that there might be no other kinetic limitations in this case, the described percolating network could successfully be used in the investigation of other disordered systems of interest.

B. Phosphate based cathodes

A desire to reduce costs and potential environmental impact has led to the development of lower capacity, cheaper cathode materials based on olivine-structured Li_2FePO_4 and related compounds.¹⁸⁷ These materials have long been known for their relatively high levels of ionic diffusion; however, the discovery of significant levels of electronic conductivity following minor doping with aliovalent transition metal cations has led to their adoption for cathode materials.¹⁸⁸ Significant improvements to charging and discharge rates have been achieved through reducing the size of the particles in order to increase the effective working volume,^{189,190} however, diffusion into and out of the cathode remains a significant barrier to their use in many applications.¹⁹¹

The olivine structure, shown in Fig. 8, is based on interlinked MO_4 tetrahedra which form an extended three-dimensional array linked by octahedrally coordinated Fe ions. The stronger, covalent $M\text{-O}$ bonds lend olivine-structured oxides greater thermal stability and tolerance to repeated charge and discharge cycles than layered structures such as Li_xCoO_2 . Atomic scale simulations have been used to study the diffusion mechanism¹⁹² which was then subsequently confirmed by maximum entropy refinement of neutron diffraction data.¹⁹³ The Li ions are arranged in lines along the b -axis and migration takes place along this direction although following a distinctly curved path. A direct comparison with Na-ion diffusion identified a similar mechanism but with a lower activation energy for migration.¹⁹⁴

The difficulty of the use of olivine structured LiFePO_4 cathodes is the fragility of the one-dimensional diffusion, which in contrast to the two-dimensional diffusion in layered compounds, is easily interrupted by crystal defects. It also requires preferential alignment of the crystal planes to the surface of the crystallites and favours smaller, higher purity particles to optimise the intercalation/decalcation reaction. The surface chemistry of the LiFePO_4 particles is complex; however, atomic scale simulations are able to provide an estimate of the surface energies,¹⁹⁵ which can be used to explain the occurrence of different surface fractions depending on the method of chemical synthesis.^{196–198}

C. Electrolyte developments

In traditional rechargeable Li-ion batteries, intercalation in the cathode is the limiting design feature leading to a limited capacity after many charge and discharge cycles. However, along with renewed interest in alternative battery technologies, Li-sulphur or Li-air, which with pure Li foil cathodes have a theoretical capacity of 3600 mAh/g, have driven interest in higher diffusivity electrodes as well.

Although polymeric materials and glasses have been proposed as electrolytes, nonetheless ceramic materials, and particularly oxides and perovskites, can be considered as

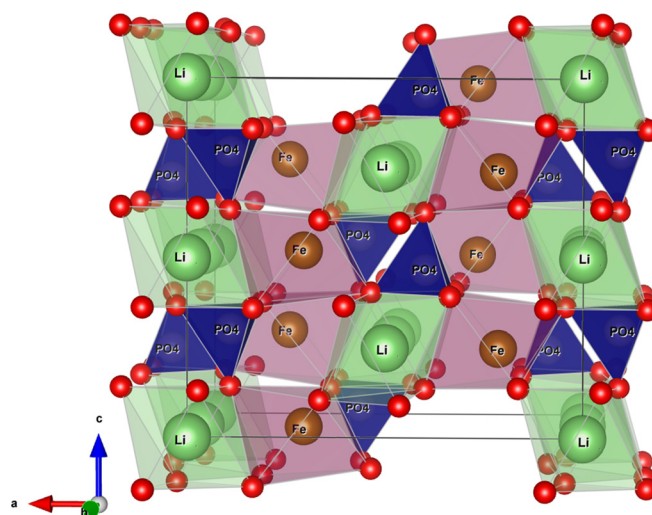


FIG. 8. A $1 \times 1 \times 2$ supercell of the olivine structured LiFePO_4 showing oxygen atoms in red, phosphate groups in blue, Fe ions in orange, and Li atoms in green. Li diffusion occurs through the chains of sites aligned with the b -axis.

advantageous for these applications. Recently Jay *et al.*¹⁹⁹ referred that the lithium lanthanum titanates such as $\text{La}_{2/3-x}\text{Li}_x\text{TiO}_3$ (LLTO), as structural disordered materials, are very interesting due to their high ionic conductivities and their non-Arrhenius behaviour. The main insights gained by MD in this particular material have to do with the extended analysis of the 3D network of diffusion pathways through which the ions can move in various directions.

It was previously determined by Ohnishi *et al.*²⁰⁰ that the cations of the perovskite tend to form low La content (La_{poor}) and high La content (La_{rich}) atomic layers that affect the Li ionic migration. This can be described by the ordering degree in the crystal using the following equation:¹⁹⁹

$$S = \frac{R_{\text{La-rich}} - R_{\text{dis.}}}{1 - R_{\text{dis.}}},$$

where the $R_{\text{dis.}}$ and $R_{(\text{La-rich})}$ terms are the occupancies of the A -sites by the exact amount of La^{3+} ions for the disordered and the La-rich layered structures, respectively. Figure 9 is a schematic representation of LLTO where layers with La_{poor} and La_{rich} are coloured in blue and yellow, respectively. It was calculated by Jay *et al.* that in the case where $S = 0$ (the system's structure is completely disordered) the ionic diffusion is completely homogeneous and isotropic. This is because the diffusion in LLTO is facilitated by vacancies; consequently, the total stoichiometry and the ordering degree that leads to the percolating network (Fig. 9) are important. The structure and its impact on the conductivity of LLTO were then studied using an advanced methodology based on MD combined with a Genetic Algorithm (GA). This approach successfully replicated the experimentally determined results,¹⁷⁴ whereas it provides a way to tailor layers in such a way that Li diffusivity is maximised. As this method is transferable it can pave the way to design disordered materials with optimum properties for energy applications. This is an example where advanced modelling techniques not only act synergistically with experiment but can also provide unique insights.

Li ion diffusion channels have also been described by Kim *et al.*²⁰¹ for the case of the monoclinic LiMnBO_3 , illustrated in Fig. 10. It was strongly suggested that the intercalation kinetic processes are affected significantly by cation disorder in the material. They investigated the atomic effects by using both computational and experimental techniques. The single dimensional (1D) transport properties of LiMnBO_3 are considered to be unusual and can be influenced by the particle size of the material. In particular, it was determined that the electrochemical performance can be improved through the particle nanosizing and the structural stabilization. Additionally, the experimental observation of a diffusivity limitation leads to the relative discrepancy between the theoretical prediction and the physical processes. Kim *et al.*²⁰¹ investigated the Mn/Li structural disorder of LiMnBO_3 with the conclusions linked to the diffusion limitation of the Li ions which was due to channel blocking. For a completely isotropic distribution of Mn_{Li} antisites in the crystal, it was shown that particles of a larger size will be more affected by the channel blocking. Importantly, the total diffusivity of a system can be influenced by external stimuli on the particles. For example, the smaller particles can be activated under external voltage/current conditions responding faster than the larger particles. In this framework, particle size distribution will be linked to the distribution of various diffusivities. Kim *et al.* observed that during the several charge/discharge reactions, the Li ion diffusivity decreases. Through the manipulation of the chemistry in the system, it

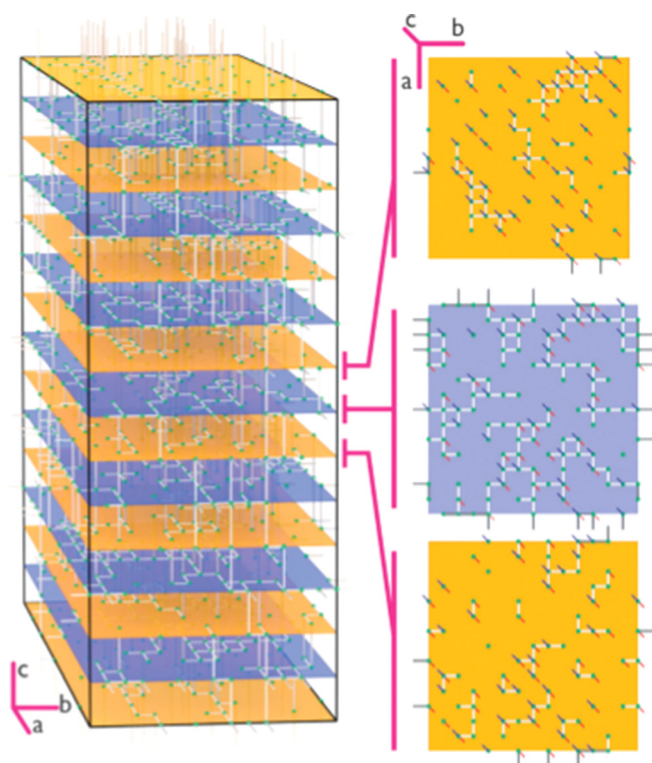


FIG. 9. LLTO schematic graph where the pathways in ab directions are shown for every La_{poor} and La_{rich} layer. The structure has been optimized using MD in conjunction with GA. Reproduced with permission from Jay *et al.*, Phys. Chem. Chem. Phys. 17, 178 (2015).¹⁹⁹ Copyright 2015 Royal Society of Chemistry.

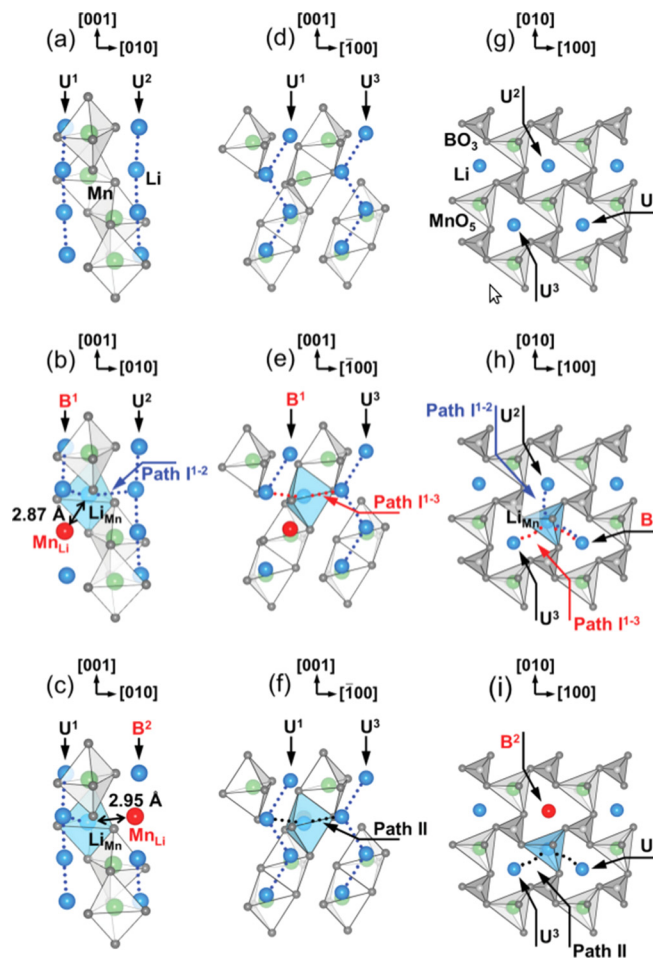


FIG. 10. The Li pathways visualized using DFT calculations along the (a)–(c) [100], (d)–(f) [010], and (g)–(i) [001] directions in LiMnBO_3 . In this figure, (a), (d), and (g) correspond to no antisite disorder, (b), (e), and (h) to antisite disorder to the lowest formation energy (0.747 eV), and (c), (f), and (i) to the second lowest formation energy (0.752 eV). U and B refer to the unblocked and blocked channels, respectively, whereas superscripts label the channel positions. Reproduced with permission from Kim *et al.*, Adv. Energy Mater. 5, 1401916 (2015).²⁰¹ Copyright 2015 John Wiley and Sons.

could be possible to minimize the kinetics limitations and unblock the channels leading to the Li ion extraction.

D. MXenes

Two-dimensional materials such as MXenes have recently emerged to gain the attention as potential candidates for Li-ion batteries, due to the combination of high charging rates and attractive ionic capacity.^{175,202–204} This new group of materials includes transition metal carbides as well as carbonitrides that can be formed by the etching of the A metal from the $M_{n+1}AX_n$ phases (where $n = \text{integer}$, $M = \text{transition metal}$, $A = \text{group of 13–16 elements}$, $X = \text{C or N}$).²⁰² Numerous MXenes have been discovered during the last few years^{175,203} with the titanium carbides being by far the most common in the literature. Nevertheless, several MXenes with $M = \text{Ta, V and Nb}$ can also be important.

Soon after their discovery, MXenes were shortlisted for numerous applications including catalysts, sensors, supercapacitors and Li-ion batteries.^{204,205} Regarding Li-battery

anode materials the V_2C -based (as well as the Ti_2C and Nb-based) MXenes are the most promising, whereas for electrode materials Ti_2C , $Ti_{0.5}$, $Nb_{0.5}C$, and T_3CN .^{205–209} For example, Zhao *et al.*²⁰⁹ investigated the potential of the energy storage of several MXenes including Ti_2C which was proposed as an anode material, whereas Berdiyrov²¹⁰ theoretically studied the Ti_3C_2 MXene to provide information on the Na and Li absorption on the electronic transport properties of the material. Here, we will focus on the Nb-based MXenes and describe the mechanism and energetics of Li diffusion.

Nb_2C and Nb_2CX_2 have been investigated by Zhu *et al.*²⁰² who employed DFT to investigate the defect process of Li. DFT calculations were deemed to be in good agreement with experimental results^{211,212} regarding the lattice constants and bond lengths. Using DFT, the analysis of every particular structure led to the most energetically favourable site for the adsorbed Li atoms, which is the top of the C atom.¹⁶⁰

Figure 11 reports the migration pathways and diffusion barriers for Li on Nb_2C and Nb_2CX_2 ($X = O$ and F). The 3 possible migration pathways considered for Li diffusion are from top of C to the most stable nearest neighbour [i.e., (I) C-C, (II) C-Nb(2)/O/F-C and (III) C-Nb(1)-C]. Pathway II has the lowest diffusion barrier of 0.036 eV for pristine Nb_2C . For the passivated substrates, the lowest diffusion barriers are along pathway III with 0.30 eV and 0.23 eV for O^- and F^- terminations, respectively. Therefore, in the pristine Nb_2C the Li ions are predicted to migrate easily with a very small diffusion barrier, however, the functionalization groups are calculated to increase the diffusion barrier considerably obstructing Li migration. This in turn can be a problem in numerous 2D materials where the Li diffusion will be higher when functional groups are introduced and might hinder their application.

VI. SUMMARY AND CONCLUSIONS

Diffusion is a phenomenon that is critically important for the development of more efficient SOFCs and batteries. The present review has focused on the role of atomic scale models to predict and investigate the oxygen and lithium diffusion mechanisms in energy materials in these electrochemical cells. It is anticipated that in conjunction with validation and verification experiments these computational modelling approaches will become increasingly important and will impact the community by the replacement of more empirical qualitative arguments in the discovery of energy materials. Advanced materials, which are designed rather than chosen for a given application, contain too many possible permutations of composition and structure to be usefully explored using traditional chemical synthesis. Therefore, predictive modelling in order to provide a rational survey of the composition phase space or well-founded, clear design principles is a prerequisite to accelerate their adoption.

We note two important modern developments in material physics which we believe may have significant impact on the future performance of fuel cells and battery materials. The first is the increasing use of layered heterostructures to

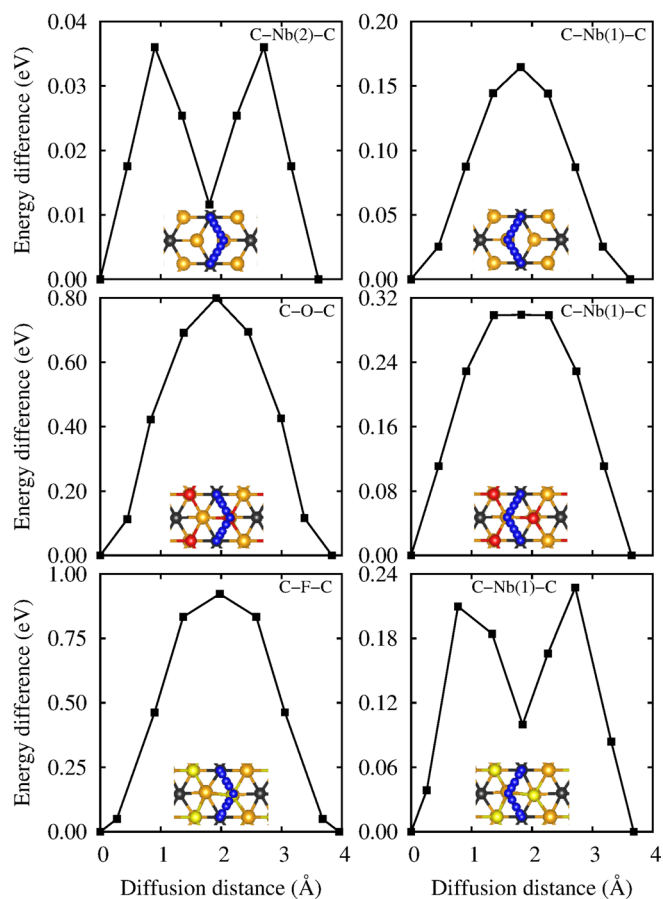


FIG. 11. Diffusion barrier profiles of Li on Nb_2C and Nb_2CX_2 ($X = O$ and F) and corresponding migration pathways for Li diffusion. The Nb, C, O, F, and Li atoms are shown in brown, black, red, yellow, and blue colour.

impose strain within a crystal lattice and the second is the rapid progress that is being made in computational material design.

A. Strain and interface design

As discussed in Sec. III A, the use of strain has already been identified as an important controlling parameter in diffusivity in ceria. Introducing artificial lattice strain through chemical heterogeneity in the microstructure may provide a route to increase diffusivity in both SOFC and batteries.²¹³ However, the presence of these interfaces may also provide a source or sink of defects allowing deviations from stoichiometry. As an example, recent work on pulsed laser deposited Sr-doped lanthanum manganite has shown significant enhancement of oxygen diffusivity at low temperatures due to the presence of the interface between this and the underlying electrode substrate.²¹⁴ This is attributed to both the strain within the layers and also the boundary itself providing a source of oxygen interstitials. The thermodynamics and kinetics of point defect behaviour near to chemically sharp interfaces may be dramatically different to that in bulk materials. Ironically, as the fabrication techniques to produce these new interfaces become more exacting, the simulations become simpler and more direct as the length-scales approach the atomic scale. We foresee a significant and

corroborative role for atomic scale modelling in understanding these structures.

New materials for both fuel cells and batteries will increasingly make use of compositionally or structurally graded nanoscale interfaces. Strain is endemic in these materials due to the deliberately induced mismatch in lattice parameter, and equally importantly, the largely unavoidable differential thermal expansion across heterophase boundaries. Management of the beneficial and deleterious effects of epitaxial strain on diffusion will therefore be an important part of future device manufacture. The method of calculating diffusivity from atomic scale simulations will provide clear guidance as the measurement of these interface regions is beset by problems of separating the genuine contribution to atomic mobility due to strain from either electrical conductivity in the substrate or chemical segregation to the boundary. Strains on an atomic scale can be accounted for in a formal context, for example, the strain dipole method which shows promise for predicting modification to diffusivity for an arbitrary triaxial stress state.²¹⁵

B. Computational material discovery

Traditional materials science is built on compounds that have evolved over many years through iterative changes to their composition and processing parameters. This process has been guided by prior knowledge some of which is based on sound theoretical grounds (the periodic table for example) and some is more heuristic. This is a slow and not necessarily effective way of choosing an optimum material for a given application. Computational materials discovery is the use of first principles calculations to rapidly and cheaply predict properties for a range of composition and structures in order to speed up this exploration rate. This is a recent and evolving field but already it is producing notable results. In Sec. V A, it was discussed that the specific composition of the Li-rich disordered rocksalt compound was synthesised only after DFT calculations identified the composition and disorder parameter as having particularly favourable Li-diffusion characteristics. Similar cation-disordered oxide structures containing novel combinations of metal cations²¹⁶ have shown a number of remarkable properties,²¹⁷ including reports of room temperature superionic behaviour for Li-ion conduction.²¹⁸ Again, DFT supported through the use of the semiquasirandom (SQS) method²¹⁹ to mimic cation disorder in small supercells has been used to enable rapid exploration and discovery of the very wide phase space available to these materials.²²⁰

Despite advancing computer power, it is no more possible to calculate the properties of all possible element combinations for even a modestly complex crystal system than it is to experimentally synthesise and test them (although the calculations would progress much faster). The usefulness of these methods therefore relies upon regression of these properties into features,²²¹ which could represent bond lengths, compositions, or any structural parameter, and then, the use of these features to make an informed guess as to where to target the next set of calculations. This allows the dataset to be built intelligently, efficiently and with a focus on the most

promising compounds. Although not directly calculating diffusion, a number of studies have successfully applied these methods to characterise possible materials for Li-battery anodes and cathodes.^{222–224} Similarly, the structure and properties of the apatites and MAX-phases (the chemical precursor to the MXenes discussed in Sec. V D) have been examined using these methods.^{225,226}

C. Concluding remarks

In this review, we have highlighted the use of atomic scale models in identifying the governing dynamics of diffusion in two classes of energy materials. There are several areas where these models can provide rapid, cheap characterisation of diffusion rates and activation energies and these will be increasingly important as modern materials become complex and tailored to individual applications. Because the energy materials considered here have large values of diffusivity they will be amongst the first areas to benefit from this approach, but similar techniques are likely to be useful across several different areas of energy material research.

What is the future of atomic scale simulations in this area? We can be almost certain that there will be a continued growth in the availability of computing power which will enable larger and longer time simulations. The field is currently populated by a wide range of individuals and groups of researchers, rather than a handful of labs with access to national-scale computing facilities, which suggests that growth in available computer power is meeting the needs of the community. We do foresee requirements for more intelligent analysis methods: as simulations become larger, they will also become increasingly cumbersome. For example, methods for automatically identifying the transition states that makeup a diffusion pathway will be required in order to extract meaningful information from large simulations of complex crystal structures, it will no longer be possible to do this by inspection of the MD trajectories which may reach many gigabytes of raw data. We also highlight the recent endeavours to provide an open repository for simulation data^{222,227,228} that should provide a significant improvement to the transferability and validation of simulation data, together with tools for the wider experimental community to access modelling results in a consistent and comprehensible format.

Despite the recent interest in developing automated discovery and design of materials, we stress that there is still synergy between these models and experimental data generated from more traditional material science. It is significantly easier to calculate an ionic density distribution or activation energy from a simulation for comparison with experimental data than it is to unpick an experiment to provide a time and spatially resolved crystallographic model. The use of these simulations can therefore articulate theories of bonding and diffusion which are absent from the more abstract point and group language of modern crystallography. We therefore see a continued importance of atomic scale models in interpreting and providing a common understanding of experimental data.

ACKNOWLEDGMENTS

The authors thank Professor Robin Grimes and Professor John Kilner of Imperial College London for useful discussions. A.C. is grateful for funding from the Lloyd's Register Foundation, a charitable foundation helping to protect life and property by supporting engineering-related education, public engagement and the application of research.

- ¹M. Born and R. Oppenheimer, *Ann. Phys.* **389**, 457 (1927).
- ²M. Born and K. Huang, *Dynamical Theory of Crystal Lattices* (Clarendon Press, 1998).
- ³R. Hempelmann, *J. Less Common Met.* **101**, 69 (1984).
- ⁴R. Potyrailo, K. Rajan, K. Stoeve, I. Takeuchi, B. Chisholm, and H. Lam, *ACS Comb. Sci.* **13**, 579 (2011).
- ⁵S. Curtarolo, G. L. W. Hart, M. B. Nardelli, N. Mingo, S. Sanvito, and O. Levy, *Nat. Mater.* **12**, 191 (2013).
- ⁶S. C. Singhal, *Solid State Ionics* **135**, 305 (2000).
- ⁷B. C. Steele and A. Heinzl, *Nature* **414**, 345 (2001).
- ⁸N. Q. Minh and T. Takahashi, *Science and Technology of Ceramic Fuel Cells* (Elsevier Science, 1995).
- ⁹J. Fleig, *Annu. Rev. Mater. Res.* **33**, 361 (2003).
- ¹⁰A. J. Jacobson, *Chem. Mater.* **22**, 660 (2010).
- ¹¹A. Tarancón, *Energies* **2**, 1130 (2009).
- ¹²J. B. Goodenough, *Annu. Rev. Mater. Res.* **33**, 91 (2003).
- ¹³A. Aguadero, L. Fawcett, S. Taub, R. Woolley, K.-T. Wu, N. Xu, J. A. Kilner, and S. J. Skinner, *J. Mater. Sci.* **47**, 3925 (2012).
- ¹⁴A. Tarancón, M. Burriel, J. Santiso, S. J. Skinner, and J. A. Kilner, *J. Mater. Chem.* **20**, 3799 (2010).
- ¹⁵S. B. Adler, J. A. Lane, and B. C. H. Steele, *J. Electrochem. Soc.* **143**, 3554 (1996).
- ¹⁶S. B. Adler, *Solid State Ionics* **111**, 125 (1998).
- ¹⁷W. C. Chueh and S. M. Haile, *Annu. Rev. Chem. Biomol. Eng.* **3**, 313 (2012).
- ¹⁸J. Motavalli, *Nature* **526**, S96 (2015).
- ¹⁹J.-M. Tarascon, *Philos. Trans. R. Soc. London A* **368**, 3227 (2010).
- ²⁰J. Lee, A. Urban, X. Li, D. Su, G. Hautier, and G. Ceder, *Science* **343**, 519 (2014).
- ²¹R. A. De Souza and J. Maier, *Phys. Chem. Chem. Phys.* **5**, 740 (2003).
- ²²A. Predith, G. Ceder, C. Wolverton, K. Persson, and T. Mueller, *Phys. Rev. B Condens. Matter* **77**, 144104 (2008).
- ²³S. Hull, *Rep. Prog. Phys.* **67**, 1233 (2004).
- ²⁴J. B. Boyce and B. A. Huberman, *Phys. Rep.* **51**, 189 (1979).
- ²⁵F. A. Kröger and H. J. Vink, in *Solid State Physics*, edited by F. Seitz and D. Turnbull (Academic Press, 1956), pp. 307–435.
- ²⁶M. Youssef and B. Yildiz, *Phys. Rev. B Condens. Matter* **86**, 144109 (2012).
- ²⁷M. Nolan, J. E. Fearon, and G. W. Watson, *Solid State Ionics* **177**, 3069 (2006).
- ²⁸H. L. Tuller and P. K. Moon, *Mater. Sci. Eng. B* **1**, 171 (1988).
- ²⁹K. J. Laidler and M. C. King, *J. Phys. Chem.* **87**, 2657 (1983).
- ³⁰D. Marrocchelli, S. R. Bishop, H. L. Tuller, and B. Yildiz, *Adv. Funct. Mater.* **22**, 1958 (2012).
- ³¹J. A. Kilner and R. J. Brook, *Solid State Ionics* **6**, 237 (1982).
- ³²J. R. Tolchard, P. R. Slater, and M. S. Islam, *Adv. Funct. Mater.* **17**, 2564 (2007).
- ³³S. Hull, D. A. Keen, D. S. Sivia, and P. Berastegui, *J. Solid State Chem.* **165**, 363 (2002).
- ³⁴M. Yashima, in *Perovskite Oxide for Solid Oxide Fuel Cells*, edited by T. Ishihara (Springer US, 2009), pp. 117–145.
- ³⁵A. Rikitin and M. Kobayashi, *Phys. Rev. B Condens. Matter* **53**, 3088 (1996).
- ³⁶M. Aniya, *Solid State Ionics* **70**, 673 (1994).
- ³⁷Y. Kowada, Y. Yamada, M. Tatsumisago, T. Minami, and H. Adachi, *Solid State Ionics* **136–137**, 393 (2000).
- ³⁸C. Satheesan Babu and B. L. Tembe, *Chem. Phys. Lett.* **194**, 351 (1992).
- ³⁹W. Kohn and L. J. Sham, *Phys. Rev.* **140**, A1133 (1965).
- ⁴⁰P. Hohenberg and W. Kohn, *Phys. Rev.* **136**, B864 (1964).
- ⁴¹J. P. Perdew, J. A. Chevary, S. H. Vosko, K. A. Jackson, M. R. Pederson, D. J. Singh, and C. Fiolhais, *Phys. Rev. B: Condens. Matter* **48**, 4978 (1993).
- ⁴²J. P. Perdew, J. A. Chevary, S. H. Vosko, K. A. Jackson, M. R. Pederson, D. J. Singh, and C. Fiolhais, *Phys. Rev. B: Condens. Matter* **46**, 6671 (1992).
- ⁴³J. P. Perdew, K. Burke, and M. Ernzerhof, *Phys. Rev. Lett.* **77**, 3865 (1996).
- ⁴⁴A. E. Mattsson, P. A. Schultz, M. P. Desjarlais, T. R. Mattsson, and K. Leung, *Modell. Simul. Mater. Sci. Eng.* **13**, R1 (2004).
- ⁴⁵J. P. Perdew, M. Ernzerhof, and K. Burke, *J. Chem. Phys.* **105**, 9982 (1996).
- ⁴⁶V. I. Anisimov VI, J. Zaanen, and O. K. Andersen, *Phys. Rev. B: Condens. Matter* **44**, 943 (1991).
- ⁴⁷V. I. Anisimov, F. Aryasetiawan, and A. I. Lichtenstein, *J. Phys. Condens. Matter* **9**, 767 (1999).
- ⁴⁸S. L. Dudarev, G. A. Botton, S. Y. Savrasov, C. J. Humphreys, and A. P. Sutton, *Phys. Rev. B: Condens. Matter* **57**, 1505 (1998).
- ⁴⁹D. Gryaznov, E. Blokhin, A. Sorokine, E. A. Kotomin, R. A. Evarestov, A. Bussmann-Holder, and J. Maier, *J. Phys. Chem. C* **117**, 13776 (2013).
- ⁵⁰D. Fuks, Y. Mastrikov, E. Kotomin, and J. Maier, *J. Mater. Chem. A Mater. Energy Sustainability* **1**, 14320 (2013).
- ⁵¹N. Sandberg and R. Holmestad, *Phys. Rev. B Condens. Matter* **73**, 014108 (2006).
- ⁵²M. Mantina, S. L. Shang, Y. Wang, L. Q. Chen, and Z. K. Liu, *Phys. Rev. B Condens. Matter* **80**, 184111 (2009).
- ⁵³Y.-L. Lee, D. Morgan, J. Kleis, and J. Rossmeisl, *ECS Trans.* **25**, 2761 (2009).
- ⁵⁴W.-W. Liu, D. Wang, Z. Wang, J. Deng, W.-M. Lau, and Y. Zhang, *Phys. Chem. Chem. Phys.* **19**, 6481 (2017).
- ⁵⁵M. Youssef and B. Yildiz, *Phys. Rev. B Condens. Matter* **89**, 024105 (2014).
- ⁵⁶A. M. Ritzmann, A. B. Muñoz-García, M. Pavone, J. A. Keith, and E. A. Carter, *Chem. Mater.* **25**, 3011 (2013).
- ⁵⁷M. Fuchs and M. Scheffler, *Comput. Phys. Commun.* **119**, 67 (1999).
- ⁵⁸H. J. Monkhorst and J. D. Pack, *Phys. Rev. B Condens. Matter* **13**, 5188 (1976).
- ⁵⁹J. C. Phillips, *Rev. Mod. Phys.* **42**, 317 (1970).
- ⁶⁰L. Pauling, *J. Am. Chem. Soc.* **54**, 988 (1932).
- ⁶¹J. B. Gibson, A. N. Goland, M. Milgram, and G. H. Vineyard, *Phys. Rev.* **120**, 1229 (1960).
- ⁶²F. H. Stillinger and A. Rahman, *J. Chem. Phys.* **60**, 1545 (1974).
- ⁶³A. Rahman, *Phys. Rev.* **136**, A405 (1964).
- ⁶⁴K. T. Butler, J. M. Frost, J. M. Skelton, K. L. Svane, and A. Walsh, *Chem. Soc. Rev.* **45**, 6138 (2016).
- ⁶⁵M. Born and J. E. Mayer, *Z. Phys.* **75**, 1 (1932).
- ⁶⁶R. A. Buckingham, *Proc. R. Soc. London A: Math., Phys. Eng. Sci.* **168**, 264 (1938).
- ⁶⁷F. G. Fumi and M. P. Tosi, *J. Phys. Chem. Solids* **25**, 31 (1964).
- ⁶⁸M. P. Tosi and F. G. Fumi, *J. Phys. Chem. Solids* **25**, 45 (1964).
- ⁶⁹C. R. A. Catlow, *Computer Modelling in Inorganic Crystallography* (Academic Press, San Diego, Boston, 1997).
- ⁷⁰M. W. D. Cooper, M. J. D. Rushton, and R. W. Grimes, *J. Phys. Condens. Matter* **26**, 105401 (2014).
- ⁷¹J. Yu, S. B. Sinnott, and S. R. Phillpot, *Phys. Rev. B Condens. Matter* **75**, 085311 (2007).
- ⁷²T.-R. Shan, B. D. Devine, T. W. Kemper, S. B. Sinnott, and S. R. Phillpot, *Phys. Rev. B Condens. Matter* **81**, 125328 (2010).
- ⁷³A. C. T. van Duin, B. V. Merinov, S. S. Jang, and W. A. Goddard III, *J. Phys. Chem. A* **112**, 3133 (2008).
- ⁷⁴S. M. Woodley, J. D. Gale, P. D. Battle, and C. R. A. Catlow, *J. Chem. Phys.* **119**, 9737 (2003).
- ⁷⁵J. A. Martinez, D. E. Yilmaz, T. Liang, S. B. Sinnott, and S. R. Phillpot, *Curr. Opin. Solid State Mater. Sci.* **17**, 263 (2013).
- ⁷⁶L. Sun, D. Marrocchelli, and B. Yildiz, *Nat. Commun.* **6**, 6294 (2015).
- ⁷⁷A. F. Voter, F. Montalenti, and T. C. Germann, *Annu. Rev. Mater. Res.* **32**, 321 (2002).
- ⁷⁸D. C. Rapaport, R. L. Blumberg, S. R. McKay, W. Christian, and Others, *Comput. Phys.* **10**, 456 (1996).
- ⁷⁹G. Henkelman and H. Jónsson, *J. Chem. Phys.* **113**, 9978 (2000).
- ⁸⁰G. Henkelman, B. P. Uberuaga, and H. Jónsson, *J. Chem. Phys.* **113**, 9901 (2000).
- ⁸¹N. Govind, M. Petersen, G. Fitzgerald, D. King-Smith, and J. Andzelm, *Comput. Mater. Sci.* **28**, 250 (2003).
- ⁸²J. R. Tolchard, M. S. Islam, and P. R. Slater, *J. Mater. Chem.* **13**, 1956 (2003).

- ⁸³A. Chroneos, D. Parfitt, J. A. Kilner, and R. W. Grimes, *J. Mater. Chem.* **20**, 266 (2010).
- ⁸⁴D. S. D. Gunn, N. L. Allan, and J. A. Purton, *J. Mater. Chem. A Mater. Energy Sustainable* **2**, 13407 (2014).
- ⁸⁵M. R. Sorensen and A. F. Voter, *J. Chem. Phys.* **112**, 9599 (2000).
- ⁸⁶B. P. Uberuaga and L. J. Vernon, *Solid State Ionics* **253**, 18 (2013).
- ⁸⁷M. W. Finnis, A. Y. Lozovoi, and A. Alavi, *Annu. Rev. Mater. Res.* **35**, 167 (2005).
- ⁸⁸L. Wang, T. Maxisch, and G. Ceder, *Phys. Rev. B Condens. Matter* **73**, 195107 (2006).
- ⁸⁹D. Gryaznov, S. Baumann, E. A. Kotomin, and R. Merkle, *J. Phys. Chem. C* **118**, 29542 (2014).
- ⁹⁰A. Mitterdorfer and L. J. Gauckler, *Solid State Ionics* **111**, 185 (1998).
- ⁹¹R. Sayers, J. Liu, B. Rustumji, and S. J. Skinner, *Fuel Cells* **8**, 338 (2008).
- ⁹²H. Ullmann, N. Trofimenko, F. Tietz, D. Stöver, and A. Ahmad-Khanlou, *Solid State Ionics* **138**, 79 (2000).
- ⁹³C. Milliken, S. Guruswamy, and A. Khandkar, *J. Am. Ceram. Soc.* **85**, 2479 (2002).
- ⁹⁴H. L. Tuller and A. S. Nowick, *J. Electrochem. Soc.* **126**, 209 (1979).
- ⁹⁵P. P. Dholabhai, J. B. Adams, P. Crozier, and R. Sharma, *J. Chem. Phys.* **132**, 094104 (2010).
- ⁹⁶M. Nakayama, H. Ohshima, M. Nogami, and M. Martin, *Phys. Chem. Chem. Phys.* **14**, 6079 (2012).
- ⁹⁷S. J. Hong and A. V. Virkar, *J. Am. Ceram. Soc.* **78**, 433 (1995).
- ⁹⁸P. P. Dholabhai, J. B. Adams, P. Crozier, and R. Sharma, *Phys. Chem. Chem. Phys.* **12**, 7904 (2010).
- ⁹⁹D. A. Andersson, S. I. Simak, N. V. Skorodumova, I. A. Abrikosov, and B. Johansson, *Proc. Natl. Acad. Sci. U. S. A.* **103**, 3518 (2006).
- ¹⁰⁰M. Nakayama and M. Martin, *Phys. Chem. Chem. Phys.* **11**, 3241 (2009).
- ¹⁰¹Z.-P. Li, T. Mori, J. Zou, and J. Drennan, *Phys. Chem. Chem. Phys.* **14**, 8369 (2012).
- ¹⁰²M. Alaydrus, M. Sakaue, S. M. Aspera, T. D. K. Wungu, T. P. T. Linh, H. Kasai, T. Ishihara, and T. Mohri, *J. Phys. Condens. Matter* **25**, 225401 (2013).
- ¹⁰³K. Eguchi, T. Setoguchi, T. Inoue, and H. Arai, *Solid State Ionics* **52**, 165 (1992).
- ¹⁰⁴S. Omar, E. D. Wachsman, J. L. Jones, and J. C. Nino, *J. Am. Ceram. Soc.* **92**, 2674 (2009).
- ¹⁰⁵D. J. Seo, K. O. Ryu, S. B. Park, K. Y. Kim, and R.-H. Song, *Mater. Res. Bull.* **41**, 359 (2006).
- ¹⁰⁶S.-F. Wang, C.-T. Yeh, Y.-R. Wang, and Y.-C. Wu, *J. Mater. Res. Technol.* **2**, 141 (2013/4).
- ¹⁰⁷J. Faber, C. Geoffroy, A. Roux, A. Sylvestre, and P. Abélard, *Appl. Phys. A: Mater. Sci. Process.* **49**, 225 (1989).
- ¹⁰⁸V. Butler, C. R. A. Catlow, B. E. F. Fender, and J. H. Harding, *Solid State Ionics* **8**, 109 (1983).
- ¹⁰⁹L. Minervini, M. O. Zacate, and R. W. Grimes, *Solid State Ionics* **116**, 339 (1999).
- ¹¹⁰F. Ye, T. Mori, D. R. Ou, A. N. Cormack, R. J. Lewis, and J. Drennan, *Solid State Ionics* **179**, 1962 (2008).
- ¹¹¹F. Ye, T. Mori, D. R. Ou, and A. N. Cormack, *Solid State Ionics* **180**, 1127 (2009).
- ¹¹²P. P. Dholabhai, S. Anwar, J. B. Adams, P. A. Crozier, and R. Sharma, *Modell. Simul. Mater. Sci. Eng.* **20**, 15004 (2012).
- ¹¹³B. Wang, R. J. Lewis, and A. N. Cormack, *Acta Mater.* **59**, 2035 (2011/3).
- ¹¹⁴A. Ismail, J. Hooper, J. B. Giorgi, and T. K. Woo, *Phys. Chem. Chem. Phys.* **13**, 6116 (2011).
- ¹¹⁵D. R. Ou, F. Ye, and T. Mori, *Phys. Chem. Chem. Phys.* **13**, 9554 (2011).
- ¹¹⁶T.-H. Yeh and C.-C. Chou, *Phys. Scr.* **2007**, 303 (2007).
- ¹¹⁷N. Sata, K. Eberman, K. Eberl, and J. Maier, *Nature* **408**, 946 (2000).
- ¹¹⁸X. X. Guo, I. Matei, J.-S. Lee, and J. Maier, *Appl. Phys. Lett.* **91**, 103102 (2007).
- ¹¹⁹J. A. Kilner, *Nat. Mater.* **7**, 838 (2008).
- ¹²⁰W. Shen, J. Jiang, and J. L. Hertz, *RSC Adv.* **4**, 21625 (2014).
- ¹²¹J. Maier, *Solid State Ionics* **131**, 13 (2000).
- ¹²²J. Garcia-Barriocanal, A. Rivera-Calzada, M. Varela, Z. Sefrioui, E. Iborra, C. Leon, S. J. Pennycook, and J. Santamaria, *Science* **321**, 676 (2008).
- ¹²³X. Guo, *Science* **324**, 465 (2009).
- ¹²⁴M. J. D. Rushton and A. Chroneos, *Sci. Rep.* **4**, 6068 (2014).
- ¹²⁵R. A. De Souza, A. Ramadan, and S. Hörner, *Energy Environ. Sci.* **5**, 5445 (2011).
- ¹²⁶A. Goyal, S. R. Phillpot, G. Subramanian, D. A. Andersson, C. R. Stanek, and B. P. Uberuaga, *Phys. Rev. B Condens. Matter* **91**, 094103 (2015).
- ¹²⁷D. J. L. Brett, A. Atkinson, N. P. Brandon, and S. J. Skinner, *Chem. Soc. Rev.* **37**, 1568 (2008).
- ¹²⁸T. Ishihara, H. Matsuda, and Y. Takita, *J. Am. Chem. Soc.* **116**, 3801 (1994).
- ¹²⁹H. J. M. Bouwmeester, D. M. W. Otter, and B. A. Boukamp, *J. Solid State Electrochem.* **8**, 599 (2004).
- ¹³⁰S. McIntosh, J. F. Vente, W. G. Haije, D. H. A. Blank, and H. J. M. Bouwmeester, *Solid State Ionics* **177**, 1737 (2006).
- ¹³¹G. C. Mather, M. S. Islam, and F. M. Figueiredo, *Adv. Funct. Mater.* **17**, 905 (2007).
- ¹³²M. S. Khan and M. S. Islam, *J. Phys. Chem. B* **102**, 3099 (1998).
- ¹³³M. Saiful Islam, *J. Mater. Chem.* **10**, 1027 (2000).
- ¹³⁴M. Yashima, K. Nomura, H. Kageyama, Y. Miyazaki, N. Chitose, and K. Adachi, *Chem. Phys. Lett.* **380**, 391 (2003).
- ¹³⁵M. Kajitani, M. Matsuda, A. Hoshikawa, S. Harjo, T. Kamiyama, T. Ishigaki, F. Izumi, and M. Miyake, *Chem. Mater.* **17**, 4235 (2005).
- ¹³⁶M. Saiful Islam and R. Andrew Davies, *J. Mater. Chem.* **14**, 86 (2003).
- ¹³⁷P. Huang and A. Petric, *J. Electrochem. Soc.* **143**, 1644 (1996).
- ¹³⁸S. Li and B. Bergman, *J. Eur. Ceram. Soc.* **29**, 1139 (2009/4).
- ¹³⁹J. W. Fergus, *J. Power Sources* **162**, 30 (2006).
- ¹⁴⁰M. Cherry, M. S. Islam, and C. R. A. Catlow, *J. Solid State Chem.* **118**, 125 (1995).
- ¹⁴¹A. Jones and M. S. Islam, *J. Phys. Chem. C* **112**, 4455 (2008).
- ¹⁴²R. A. De Souza and J. A. Kilner, *Solid State Ionics* **106**, 175 (1998).
- ¹⁴³J. He, R. K. Behera, M. W. Finnis, X. Li, E. C. Dickey, S. R. Phillpot, and S. B. Sinnott, *Acta Mater.* **55**, 4325 (2007/8).
- ¹⁴⁴D. Gryaznov, M. W. Finnis, R. A. Evarestov, and J. Maier, *Solid State Ionics* **254**, 11 (2014/1).
- ¹⁴⁵E. Olsson, X. Aparicio-Anglès, and N. H. de Leeuw, *J. Chem. Phys.* **145**, 014703 (2016).
- ¹⁴⁶P. Erhart and K. Albe, *J. Appl. Phys.* **102**, 084111 (2007).
- ¹⁴⁷H. Hayashi, H. Inaba, M. Matsuyama, N. G. Lan, M. Dokiya, and H. Tagawa, *Solid State Ionics* **122**, 1 (1999).
- ¹⁴⁸E. Boehm, J. Bassat, P. Dordor, F. Mauvy, J. Grenier, and P. Stevens, *Solid State Ionics* **176**, 2717 (2005).
- ¹⁴⁹H. Zhao, Q. Li, and L. Sun, *Sci. China Chem.* **54**, 898 (2011).
- ¹⁵⁰Y. H. Lim, J. Lee, J. S. Yoon, C. E. Kim, and H. J. Hwang, *J. Power Sources* **171**, 79 (2007).
- ¹⁵¹R. Sayers, R. A. De Souza, J. A. Kilner, and S. J. Skinner, *Solid State Ionics* **181**, 386 (2010).
- ¹⁵²A. Kushima, D. Parfitt, A. Chroneos, B. Yildiz, J. A. Kilner, and R. W. Grimes, *Phys. Chem. Chem. Phys.* **13**, 2242 (2011).
- ¹⁵³D. Parfitt, A. Chroneos, J. A. Kilner, and R. W. Grimes, *Phys. Chem. Chem. Phys.* **12**, 6834 (2010).
- ¹⁵⁴M. Yashima, M. Enoki, T. Wakita, R. Ali, Y. Matsushita, F. Izumi, and T. Ishihara, *J. Am. Chem. Soc.* **130**, 2762 (2008).
- ¹⁵⁵S. M. Aspera, M. Sakaue, T. D. K. Wungu, M. Alaydrus, T. P. T. Linh, H. Kasai, M. Nakanishi, and T. Ishihara, *J. Phys. Condens. Matter* **24**, 405504 (2012).
- ¹⁵⁶A. Perrichon, A. Piovano, M. Boehm, M. Zbiri, M. Johnson, H. Schober, M. Ceretti, and W. Paulus, *J. Phys. Chem. C* **119**, 1557 (2015).
- ¹⁵⁷A. Piovano, A. Perrichon, M. Boehm, M. R. Johnson, and W. Paulus, *Phys. Chem. Chem. Phys.* **18**, 17398 (2016).
- ¹⁵⁸A. Chroneos, B. Yildiz, A. Tarancón, D. Parfitt, and J. A. Kilner, *Energy Environ. Sci.* **4**, 2774 (2011).
- ¹⁵⁹S. Nakayama, T. Kageyama, H. Aono, and Y. Sadaoka, *J. Mater. Chem.* **5**, 1801 (1995).
- ¹⁶⁰S. Nakayama and M. Sakamoto, *J. Eur. Ceram. Soc.* **18**, 1413 (1998).
- ¹⁶¹E. Kendrick, J. E. H. Sansom, J. R. Tolchard, M. S. Islam, and P. R. Slater, *Faraday Discuss.* **134**, 181 (2007).
- ¹⁶²J. E. H. Sansom, D. Richings, and P. R. Slater, *Solid State Ionics* **139**, 205 (2001).
- ¹⁶³E. Kendrick, M. S. Islam, and P. R. Slater, *Chem. Commun.* **2008**, 715.
- ¹⁶⁴L. León-Reina, E. R. Losilla, M. Martínez-Lara, S. Bruque, and M. A. G. Aranda, *J. Mater. Chem.* **14**, 1142 (2004).
- ¹⁶⁵J. E. H. Sansom, J. R. Tolchard, M. Saiful Islam, D. Apperley, and P. R. Slater, *J. Mater. Chem.* **16**, 1410 (2006).
- ¹⁶⁶R. W. Impey, M. L. Klein, and I. R. McDonald, *J. Chem. Phys.* **82**, 4690 (1985).
- ¹⁶⁷U. M. Gundusharma, C. MacLean, and E. A. Secco, *Solid State Commun.* **57**, 479 (1986).
- ¹⁶⁸E. A. Secco, *J. Solid State Chem.* **96**, 366 (1992).

- ¹⁶⁹F. Bruneval, C. Varvenne, J. P. Crocombette, and E. Clouet, *Phys. Rev. B* **91**, 024107 (2015).
- ¹⁷⁰F. Bruneval and J.-P. Crocombette, *Phys. Rev. B Condens. Matter* **86**, 140103 (2012).
- ¹⁷¹J. B. Goodenough and K.-S. Park, *J. Am. Chem. Soc.* **135**, 1167 (2013).
- ¹⁷²M. Dahbi, N. Yabuuchi, K. Kubota, K. Tokiwa, and S. Komaba, *Phys. Chem. Chem. Phys.* **16**, 15007 (2014).
- ¹⁷³J. M. Tarascon and M. Armand, *Nature* **414**, 359 (2001).
- ¹⁷⁴J. B. Goodenough and Y. Kim, *Chem. Mater.* **22**, 587 (2010).
- ¹⁷⁵C. Eames and M. S. Islam, *J. Am. Chem. Soc.* **136**, 16270 (2014).
- ¹⁷⁶M. Nishijima, T. Ootani, Y. Kamimura, T. Sueki, S. Esaki, S. Murai, K. Fujita, K. Tanaka, K. Ohira, Y. Koyama, and I. Tanaka, *Nat. Commun.* **5**, 4553 (2014).
- ¹⁷⁷K. Ozawa, *Solid State Ionics* **69**, 212 (1994).
- ¹⁷⁸K. Mizushima, P. C. Jones, P. J. Wiseman, and J. B. Goodenough, *Mater. Res. Bull.* **15**, 783 (1980).
- ¹⁷⁹M. C. Blesa, E. Moran, C. León, J. Santamaria, J. D. Tornero, and N. Menéndez, *Solid State Ionics* **126**, 81 (1999).
- ¹⁸⁰H. J. Bang, H. Joachin, H. Yang, K. Amine, and J. Prakash, *J. Electrochem. Soc.* **153**, A731 (2006).
- ¹⁸¹J. Reed, G. Ceder, and A. Van Der Ven, *Electrochem. Solid State Lett.* **4**, A78 (2001).
- ¹⁸²J. N. Reimers and J. R. Dahn, *J. Electrochem. Soc.* **139**, 2091 (1992).
- ¹⁸³M. N. Obrovac, O. Mao, and J. R. Dahn, *Solid State Ionics* **112**, 9 (1998).
- ¹⁸⁴J. Reed and G. Ceder, *Chem. Rev.* **104**, 4513 (2004).
- ¹⁸⁵K. Kang and G. Ceder, *Phys. Rev. B Condens. Matter* **74**, 094105 (2006).
- ¹⁸⁶G. Cedar, A. Van der Ven, and M. K. Aydinol, *J. Met., Mater. Miner.* **50**, 35 (1998).
- ¹⁸⁷A. K. Padhi, K. S. Nanjundaswamy, and J. B. Goodenough, *J. Electrochem. Soc.* **144**, 1188 (1997).
- ¹⁸⁸S.-Y. Chung, J. T. Bloking, and Y.-M. Chiang, *Nat. Mater.* **1**, 123 (2002).
- ¹⁸⁹H. Huang, S.-C. Yin, and L. F. Nazar, *Electrochem. Solid State Lett.* **4**, A170 (2001).
- ¹⁹⁰K. Kang, Y. S. Meng, J. Bréger, C. P. Grey, and G. Ceder, *Science* **311**, 977 (2006).
- ¹⁹¹K. Zaghbi, A. Guerfi, P. Hovington, A. Vijh, M. Trudeau, A. Mauger, J. B. Goodenough, and C. M. Julien, *J. Power Sources* **232**, 357 (2013).
- ¹⁹²M. S. Islam, D. J. Driscoll, C. A. J. Fisher, and P. R. Slater, *Chem. Mater.* **17**, 5085 (2005).
- ¹⁹³S.-I. Nishimura, G. Kobayashi, K. Ohoyama, R. Kanno, M. Yashima, and A. Yamada, *Nat. Mater.* **7**, 707 (2008).
- ¹⁹⁴R. Tripathi, S. M. Wood, M. S. Islam, and L. F. Nazar, *Energy Environ. Sci.* **6**, 2257 (2013).
- ¹⁹⁵C. A. J. Fisher and M. Saiful Islam, *J. Mater. Chem.* **18**, 1209 (2008).
- ¹⁹⁶S. Franger, F. Le Cras, C. Bourbon, C. Benoit, P. Soudan, and J. Santos-Peña, *Recent Res. Dev. Electrochem.* **8**, 225 (2005).
- ¹⁹⁷J. Chen, M. J. Vacchio, S. Wang, N. Chernova, P. Y. Zavalij, and M. S. Whittingham, *Solid State Ionics* **178**, 1676 (2008).
- ¹⁹⁸B. Ellis, W. H. Kan, W. R. M. Makahnouk, and L. F. Nazar, *J. Mater. Chem.* **17**, 3248 (2007).
- ¹⁹⁹E. E. Jay, M. J. D. Rushton, A. Choneos, R. W. Grimes, and J. A. Kilner, *Phys. Chem. Chem. Phys.* **17**, 178 (2015).
- ²⁰⁰T. Ohnishi, K. Mitsuishi, K. Nishio, and K. Takada, *Chem. Mater.* **27**, 1233 (2015).
- ²⁰¹J. C. Kim, D.-H. Seo, H. Chen, and G. Ceder, *Adv. Energy Mater.* **5**, 1401916 (2015).
- ²⁰²J. Zhu, A. Choneos, and U. Schwingenschlöggl, *Phys. Status Solidi RRL* **9**, 726 (2015).
- ²⁰³Q. Tang and Z. Zhou, *Prog. Mater. Sci.* **58**, 1244 (2013).
- ²⁰⁴X. Zhang, J. Xu, H. Wang, J. Zhang, H. Yan, B. Pan, J. Zhou, and Y. Xie, *Angew. Chem. Int. Ed.* **52**, 4361 (2013).
- ²⁰⁵Y. Gao, L. Wang, Z. Li, A. Zhou, Q. Hu, and X. Cao, *Solid State Sci.* **35**, 62 (2014/9).
- ²⁰⁶M. Naguib, M. Kurtoglu, V. Presser, J. Lu, J. Niu, M. Heon, L. Hultman, Y. Gogotsi, and M. W. Barsoum, *Adv. Mater.* **23**, 4248 (2011).
- ²⁰⁷M. Naguib, V. N. Mochalin, M. W. Barsoum, and Y. Gogotsi, *Adv. Mater.* **26**, 992 (2014).
- ²⁰⁸M. Naguib, V. Presser, D. Tallman, J. Lu, L. Hultman, Y. Gogotsi, and M. W. Barsoum, *J. Am. Ceram. Soc.* **94**, 4556 (2011).
- ²⁰⁹S. Zhao, W. Kang, and J. Xue, *J. Phys. Chem. C* **118**, 14983 (2014).
- ²¹⁰G. R. Berdiyorov, *Appl. Surf. Sci.* **359**, 153 (2015).
- ²¹¹X. Qian, Y. Li, X. He, H. Fan, and S. Yun, *J. Phys. Chem. Solids* **72**, 954 (2011/8).
- ²¹²L.-Y. Gan, Y.-J. Zhao, D. Huang, and U. Schwingenschlöggl, *Phys. Rev. B Condens. Matter* **87**, 245307 (2013).
- ²¹³C. Tealdi, J. Heath, and M. Saiful Islam, *J. Mater. Chem. A Mater. Energy Sustainable* **4**, 6998 (2016).
- ²¹⁴F. Chiabrera, A. Morata, M. Pacios, and A. Tarancón, *Solid State Ionics* **299**, 70 (2017).
- ²¹⁵G. Subramanian, D. Perez, B. P. Uberuaga, C. N. Tomé, and A. F. Voter, *Phys. Rev. B: Condens. Matter Mater. Phys.* **87**, 144107 (2013).
- ²¹⁶C. M. Rost, E. Sachet, T. Borman, A. Moballegh, E. C. Dickey, D. Hou, J. L. Jones, S. Curtarolo, and J.-P. Maria, *Nat. Commun.* **6**, 8485 (2015).
- ²¹⁷D. Béardan, S. Franger, D. Dragoe, A. K. Meena, and N. Dragoe, *Phys. Status Solidi RRL* **10**, 328 (2016).
- ²¹⁸D. Béardan, S. Franger, A. K. Meena, and N. Dragoe, *J. Mater. Chem. A Mater. Energy Sustainable* **4**, 9536 (2016).
- ²¹⁹A. Zunger, S. Wei, L. G. Ferreira, and J. E. Bernard, *Phys. Rev. Lett.* **65**, 353 (1990).
- ²²⁰A. Urban, I. Matts, A. Abdellahi, and G. Ceder, *Adv. Energy Mater.* **6**, 1600488 (2016).
- ²²¹S. Srinivasan, S. R. Broderick, R. Zhang, A. Mishra, S. B. Sinnott, S. K. Saxena, J. M. LeBeau, and K. Rajan, *Sci. Rep.* **5**, 17960 (2015).
- ²²²J. E. Saal, S. Kirklin, M. Aykol, B. Meredig, and C. Wolverton, *JOM* **65**, 1501 (2013).
- ²²³X. Qu, A. Jain, N. N. Rajput, L. Cheng, Y. Zhang, S. P. Ong, M. Brafman, E. Maginn, L. A. Curtiss, and K. A. Persson, *Comput. Mater. Sci.* **103**, 56 (2015).
- ²²⁴Y. S. Meng and M. Elena Arroyo-de Dompablo, *Energy Environ. Sci.* **2**, 589 (2009).
- ²²⁵P. V. Balachandran and K. Rajan, *Acta Crystallogr. B* **68**, 24 (2012).
- ²²⁶P. V. Balachandran, D. Xue, J. Theiler, J. Hogden, and T. Lookman, *Sci. Rep.* **6**, 19660 (2016).
- ²²⁷A. Jain, S. P. Ong, G. Hautier, W. Chen, W. D. Richards, S. Dacek, S. Cholia, D. Gunter, D. Skinner, G. Ceder, and K. A. Persson, *APL Mater.* **1**, 011002 (2013).
- ²²⁸S. Curtarolo, W. Setyawan, S. Wang, J. Xue, K. Yang, R. H. Taylor, L. J. Nelson, G. L. W. Hart, S. Sanvito, M. Buongiorno-Nardelli, N. Mingo, and O. Levy, *Comput. Mater. Sci.* **58**, 227 (2012/6).